Investigation of unplanned dilution in open stoping mining method: A case study of the Ridder-Sokolny Mine

by

ADIL BOLEGENOV

THESIS SUPERVISOR

DR. AMOUSSOU COFFI ADOKO

Thesis submitted to the School of Mining and Geosciences of Nazarbayev University in Partial Fulfillment of the Requirements for the Degree of
Bachelor of Science in Mining Engineering

Nazarbayev University
04.10.2022

ORIGINALITY STATEMENT

I, **Adil Bolegenov**, hereby declare that this submission is my own work and to the best of my knowledge it contains no materials previously published or written by another person, or substantial proportions of material which have been accepted for the award of any other degree or diploma at Nazarbayev University or any other educational institution, except where due acknowledgement is made in the thesis.

Any contribution made to the research by others, with whom I have worked at NU or elsewhere is explicitly acknowledged in the thesis.

I also declare that the intellectual content of this thesis is the product of my own work, except to the extent that assistance from others in the project's design and conception or in style, presentation and linguistic expression is acknowledged.

Signed on **04.10.2022**

_____Adil Bolegenov_____

ABSTRACT

The open stoping mining method is considered as one of the most common mining methods for steep orebodies due to its several advantages. However, open stopes are susceptible to unplanned dilution. Dilution can jeopardize the profitability of the mining operations because it increases the production cost. This has been the case in the Ridder-Sokolny mine, where large amount of unplanned dilution was observed. The thesis is aimed to characterize the unplanned dilution experienced in the Ridder-Sokolniy mine and to develop an alternative open stope design tool to the conventional ELOS graphs used in that mine. Unplanned dilution data and design parameters of 107 stopes were collected. Firstly, the performance of the ELOS method was evaluated. Next, the multinomial logistic regression model was implemented to derive probabilistic charts relating the unplanned dilution and its two key influencing factors. The results showed poor to fair agreement with the actual unplanned dilution with the ELOS method. Therefore, this design method is not reliable for unplanned dilution in Ridder-Sokolny mine. On the other hand, the proposed charts indicated that the generated probabilistic map provide desirable accuracy of 63% for estimation of unplanned dilution in stopes. It was concluded that the multinomial logistic regression charts could be used to design open stopes as they can assist in selecting the stope dimensions that would minimize unplanned dilution.

ACKNOWLEDGMENT

First of all, I would like to thank Kazzinc Corporation and Ridder-Sokolny Mine for enabling me to have an access and to utilize their mine's geological and geotechnical data in this research project. My special thanks go to the mine geotechnical engineer Miras Zhazitov for his assistance in compiling this data.

To Assistant Prof. Amoussou Coffi Adoko, my supervisor, I owe a debt of gratitude that will never be forgotten. In the end, I was able to complete my BSc thesis on time because to his encouragement and guidance.

I would like to thank my parents and my closest friends for constant support during this research project.

Table of Contents

LIST OF FIGURES

LIST OF TABLES

1. INTRODUCTION

1.1. Background/Problem Definition

Mining by open stoping method is one of the most popular systems that are used for the mining of metallic ores. According to Le Roux and Stacey, over 50% of underground metal mines all over the world use open stoping mining systems (Le Roux & Stacey, 2017). The great depth of ore bodies is accompanied by the complex morphology of the deposits, which makes mining activities difficult to some extent. The main challenge related to open stopping is the dilution problem. Dilution of the excavated ore can cause a reduction in the grade of mined material and it leads to economic losses for the company, as the product is not as valuable as it is demanded. Therefore, dilution is one of the key aggravating aspects of mining manufactures using the open stoping method.

Moreover, dilution causes some indirect costs as it unfavorably impacts the metal recoveries. It's possible that focusing efforts on waste products (rather than ore) for mill feed may result in a missed opportunity. Thus, processing facilities will be used for material processing that contributes relatively little to the ultimate production. Mining and milling capacity is usually restricted, and this capacity is influenced by ore displacement by waste products within the total mining and processing facilities (Villaescusa, 1998). Thus, it is necessary to reduce the amount of dilution of ore by waste products.

The same challenge is faced by the Ridder-Sokolny mine supervised by Kazzinc and Glencore companies. This mine is also using an underground open-stoping system for the mining of polymetallic materials since then. According to the geotechnical report provided by SRK Consulting, calculations of both planned and unplanned dilution values were performed by the use of conventional dilution calculation methods (ELOS and ELRD) (Biryuchev, 2018). Based on these results, authors have assumed that with an unstable condition of the stopes, unplanned dilution can increase the planned level of dilution by 2.1%, and in a caved stopes it can increase by an average of 4.3% in relation to the planned level. However, the real dilution values in some stopes are larger than the planned by about 1000%. For example, in the Bystrushinskaya deposit, block 95, stope 8, the planned dilution is 3.8%; however, the real dilution is equal to 53.5%. And the similar cases are more than half of studied stopes (Biryuchev, 2018). Thus, we can see that the stope reconciliation data indicated large dilution, which was contrary to the calculated dilution according to the ELOS and ELRD methods.

Moreover, there is an issue that the use of laser scanning data to assess the level of dilution by ELOS is not possible, due to the fact that there is an insufficient convergence of the actual and design contours of the stopes. However, the accumulated and collected information on the results of monitoring voids was used in geomechanical models. Thus, the calculations of the dilution obtained ELOS method may be inappropriate

In some stopes, the actual dilution is equal to or less than the planned design dilution, which is considered as acceptable. However, it is necessary to reduce the stope dilution as much as possible to improve stability and reduce adverse economic effects.

Predicting and estimating ore dilution is acknowledged to be a tough task owing to the numerous variables that must be considered at the same time. Ore dilution problems are difficult to solve because of the phenomena that follow the mining process and the range of uncertainties surrounding the geological understanding of the deposit (Diakité, 1998). Moreover, according to Henning and Mitri, sources of unplanned dilution have been linked to stope wall instability (John G Henning & Mitri, 2008). Dilution occurs when the wall has a low mechanical strength, which causes extra waste material to fail into the stope. When an individual bed or structural feature on the stope hangingwall ruptures due to overbreak, it becomes challenging to prevent the remainder of that feature from failing into the open stope. Additionally, blasting damage has a negative impact on the stope wall's stability too.

Ore dilution can only be properly regulated if detailed information on the geology of the orebody and adjacent rocks is available, as well as failure behavior analysis. Moreover, there are always a number of unknowns during the geological analysis of the deposit, which can make controlling ore dilution challenging. The main factors affecting the amount of stope dilution are stope geometry, the in-situ stress regime, exposure period, inadequate blasting, and geological features such as faults, dykes, and so on. Here, the major factor that has an impact on the total stope stability is the in-situ stress situation; consequently, the dilution issue occurs (Wang, 2004).

1.2. Objectives of the Thesis

1.2.1. Main Objectives

The aim of this research project is to investigate and to improve the unplanned dilution in the Ridder-Sokolny mine. In order to meet the aim of this study, two main objectives are delivered.

The first main objective is to characterize the unplanned dilution experienced in the Ridder-Sokolniy Mine. The second objective is to develop an alternative open stope design tool to the conventional ELOS graph.

1.2.2. Specific Objectives

The following activities were performed for completion of the first objective:

- Conduct a literature review
- Collect stope reconciliation data (compare designed and actual dilution)
- Identify the areas of the mine with higher dilution and determine the contributing factors
- Plot ELOS graph and analyze the results
- Use Multinomial Regression Analysis for dilution analysis
- Formulate recommendations to reduce dilution in Ridder-Sokolny

1.3. Justification of the R&D

In the case of the Ridder-Sokolny mine, the calculations of planned dilution show values of about 10-15%, while the actual total unplanned dilution is approximately 30-35%. There may be various sources of the problem, such as the validity of the method for dilution measurement and calculation, the correctness of the input data for calculation, or even wrong calculations of dilution done by the geotechnical department of Ridder-Sokolny mine. As a result, there are safety problems and an economic loss due to the dilution of ore and waste.

The main beneficial significance for the mining industry of Ridder-Sokolny mine is in economic aspects. The reason is that the negative economic consequences of dilution can be very significant for the profitability of the project as a whole. As a result, it is necessary to characterize the dilution problem, to verify ELOS method for dilution calculation and to find alternative stope dilution in a case of declining of ELOS method. This research can provide valid solution for further reduction of the economic losses caused by dilution to the minimum.

1.4. Scope of Work

In order to achieve the purpose of this research project, the following activities were performed:

1) To conduct a thorough literature review on the current situation on dilution estimation in open stoping mining with the advantages and limitations of conventional methods of dilution calculation.
2) To collect information on Ridder-Sokolny mine geology and geomechanical state.
3) To collect data on stope dimensions, planned and unplanned dilution estimations of Ridder-Sokolny mine.
4) Comparison and analysis of planned and unplanned dilution calculations.
5) Use of the Multinomial Logistic Regression to provide a new statistical method for estimation of planned dilution through IBM SPSS Statistics software.

2. LITERATURE REVIEW

2.1. A brief overview of Mathew's stability graph

Mathew's stability graph was introduced in 1980 and it is used for the assessment of the stability of stope wall surface in the exploitation of wide orebodies at a depth over 1000 m. In the original version of the stability graph, Mathew and his colleagues analyzed 26 case studies of open stopes in Canadian mines. Because of the limited amount of data, Potvin proposed the Modified Stability Graph based on 175 cases (Potvin, 1988). Furthermore, the graph was extended up to 400 case studies, as the data from Australian mines was introduced into the stability graph. As a result, there are various versions of the stability graph with different number of case studies. The main idea of this method is to consider two factors and use the extended graph with the database. The factors are Mathew's stability number (N) and hydraulic radius (HR) located on the y-axis and x-axis respectively (Mawdesley, Trueman, & Whiten, 2001).

The equations for obtaining stability number (N') and hydraulic radius (HR) are presented below (Feng, Wang, Bi, Jia, & Gong, 2008).

$$N' = Q * A * B * C \qquad (1)$$

$$Q' = \frac{RQD}{Jn} * \frac{Jr}{Ja} \qquad (2)$$

$$HR = \frac{Stope\ surface\ area}{Stope\ surface\ perimeter} \qquad (3)$$

where: Q' – is modified Q-system value of rock mass;

A – is a rock stress factor;

B – is a joint orientation adjustment;

C – is a design surface orientation factor;

RQD – is a Rock Quality Designation;

Jn – is a Joint Set Number;

Jr – is a Joint Roughness Number;

Ja – is a Joint Alteration Number.

According to the N' and HR values, we can recognize if the stop dimensions are stable for particular rock mass from Mathew's stability graph provided in graph 1 (the graph considers the last version of stability graph with the database of over 400 case studies). As a result of analysis, Mathews divided the stability graph into three zones to measure the stability of stope surfaces (see Figure 1):

1. **Stable Zone -** The self-supporting excavations. Dilution is predicted to be less than 10% in this zone.
2. **Potentially Unstable Zone** – Situations of localized sloughage. Sloughage can be reduced by altering the excavation plan or installing cable support. The amount of dilution in this circumstance is estimated to be between 10% and 30%.
3. **Potential Caving Zone** – Situations in which the surface is potentially unsupportable and has a high probability to fail. In other words, there will be a genuine collapse condition.

As the interception point of N' and HR falls into a stable zone, then the stope will be stable; if the point falls into failure zone, then the stope will fail; and for caving mining methods, if the point falls into caving zone, the stope will cave.

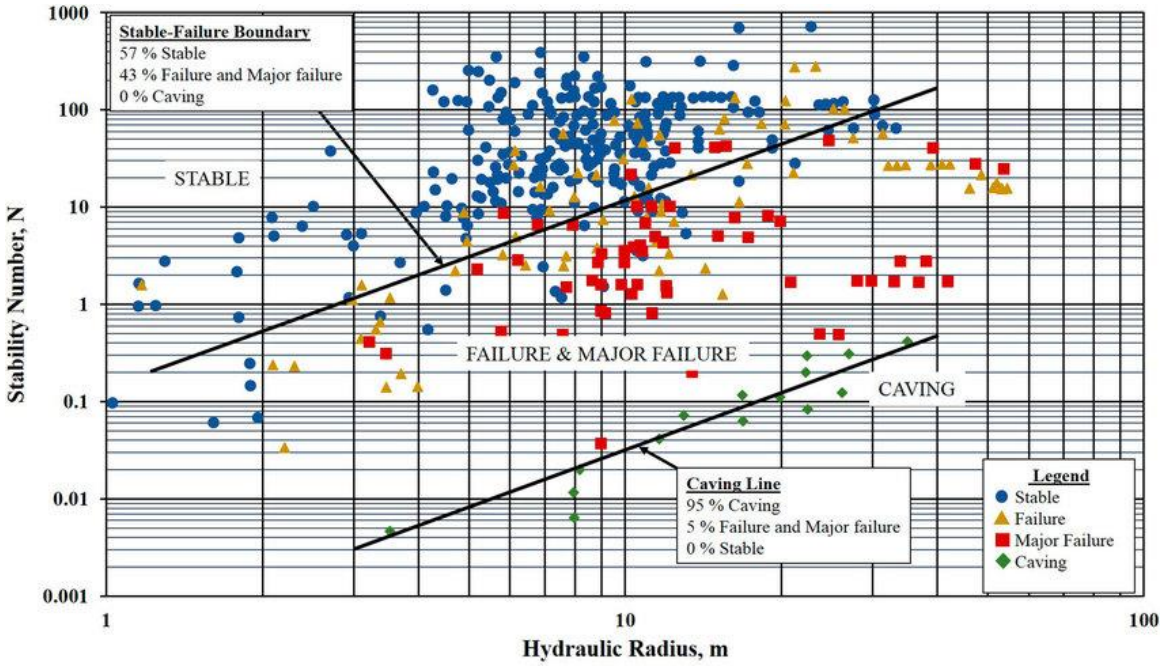

Figure 1. Extended Mathew's Stability Graph (Mawdesley et al., 2001)

Another approach of use of the stability graph is to calculate the N' value and obtain the stable stope dimension by assuming that the interception point is as close to the stable-failure boundary as possible. The reason for considering a point close to the boundary is an economical advantage as a larger stope will provide a larger portion of ore being excavated.

Even though this method has proven itself well for predicting the stability of stopes, Suorineni states that the database and transition zones of the current stability graph are inconsistent and provide low reliability on it (Suorineni, 2010). Moreover, the interpretation of the results can be different as different versions of the stability graphs can be used for stability analysis. This is accompanied by the issue of applying appropriate stability graphs for different cases as there are plenty of stability graph types (ELOS stability graphs, cablebolt design stability graph, etc.). As the application of Mathew's stability graph is an empirical way of establishing the stability of stopes, it is more convenient to calibrate the graph for each mine individually with appropriate data collection and determination of transition zones. According to Stewart and Trueman, the site specific stability graph can be created, but at least 150 case studies and 10-12 percent of intersection points should be in failure zone (Stewart & Trueman, 2001). It is worth noting that the boundaries of transition zones should be determined by statistical procedures because it will reduce the effect of bias and human error.

However, Mawdesley et al. state that there is no point in the application of statistics in stability graph determination, as no increase of accuracy degree nor reliability improvement can be achieved (Mawdesley et al., 2001). The logistic regression must be considered as the main tool for the establishment of transition zone boundaries. The only improvement of Mathew's stability graph may be done by an extension of the case study database; it will provide higher accuracy and better reliability.

2.2. Background of Dilution Analysis

There are some methods of mining, which are susceptible to contamination of ore by waste products, also referred to as dilution. Ore dilution is divided into two types: planned and unplanned. The planned dilution of the ore is determined by the rock (or ore with a reduction in grade) included in the design mining cycle. It is associated with the complexity of the morphology and thickness of the ore body, as well as the mining system. However, unplanned dilution of ore occurs due to rock falling into the stope or delamination from the contour of the

stope. The negative economic consequences of dilution can be very significant for the profitability of the project as a whole (Jang, Topal, & Kawamura, 2015).

A design of open stopes based on dilution approach was firstly studied by Pakalnis in 1986 (Pakalnis, 1986). His main approach was to measure dilution of Rutten Mine case studies. His research was unique in that he avoided using a qualitative technique to analyze sloughing or dilution and instead utilized a quantitative approach to estimate the dilution level in percent (Wang, 2004). The case histories suggested that diluting level increases with greater stope size or decreased rock quality, according to the results of investigation done by Pakalnis.

However, this method is no longer employed in the current mining industry due to several limitations. First of all, because the dilution is dependent on stope width, the approach is only suitable for stopes with the same width as those in the database, namely from 8 m to 15 m. Furthermore, although dilution originated from distinct stope surfaces, it was considered that dilution emanated from the hangingwall. Finally, because the database only contains case histories from one mine, it is skewed in terms of operational factors and ore body features specific to that mine.

2.3. A brief overview of ELOS

After research done by Pakalnis, Clark and Pakalnis were able to estimate the dilution caused by hangingwall overbreak in terms of average failure depth because to the quick development of Cavity Monitoring Systems (CMS) (L. Clark & Pakalnis, 1997). The approach that they generated for dilution analysis in stopes is Equivalent Linear Overbreak/Slough (ELOS). This method takes into consideration volumetric measurements of the stope and expresses it in terms of average depth. It is more convenient to understand the dilution in terms of depth instead of volume (L. M. Clark, 1998). The application of ELOS for dilution calculation is based on use of Mathew's stability graph and the obtained principle is called as ELOS-based stability graph; thus, the Mathew's stability number (N'), hydraulic radius (HR) and ELOS values are necessary for measurement of unplanned dilution. The values of ELOS can be obtained by the following equation:

$$ELOS = \frac{Volume\ of\ slought\ from\ stope\ surface}{Stope\ height * Wall\ strike\ length} \qquad (4)$$

Finally, all the obtained ELOS values are interpreted on the updated stability graph, which is illustrated in graph 2. This graph was obtained by Bazarbay and Adoko based on data from

Ridder-Sokolny mine in Eastern Kazakhstan (2021). Another approach of ELOS application is to use the following equation for dilution value determination (Papaioanou & Suorineni, 2016):

$$Dilution\ (\%) = \frac{ELOS}{Orebody\ width} \qquad (5)$$

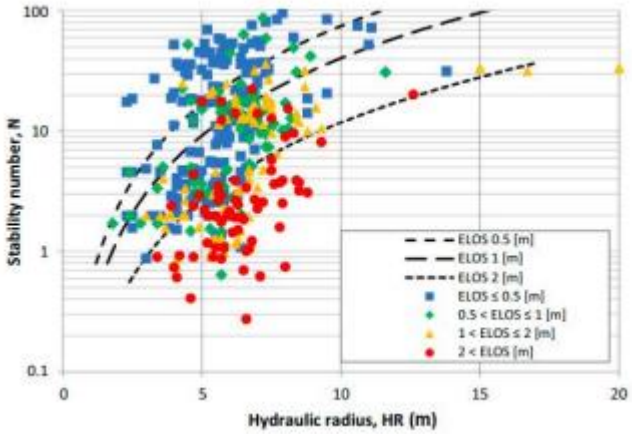

Figure 2. Updated Stability Graph (Bazarbay & Adoko, 2021)

Furthermore, Suorineni used Phase2 software by Rockscience to perform two-dimensional finite element simulations in order to indicate that the presence of a fault in rock mass increases ELOS values. For appropriate consideration of this phenomenon, he proposed the fault factor as a corrective factor to be used in the calculation of the new modified stability number (N'). As a result, when compared to the effects of the stress factor (A), joint orientation factor (B), and gravity factor (C), studies have revealed that by one to three orders of magnitude, the fault factor functions as a reduction variable for the modified stability number (N'), which suggests that the stability graph method is unreliable unless a fault factor is included during the analysis (Suorineni, 2010).

However, even though ELOS based stability graph is probably established as one of the most applicable methods for dilution calculation, there are several limitations of this method. Suorineni states that the ELOS stability graph does not differentiate its results between a vein and massive ore bodies (2010). Thus, it is proposed to produce ELOS stability graphs for both narrow vein and massive ore bodies separately, so the results of the graph are accurate and precise.

One of the most popular mining methods used for metallic ores is open stoping. According to Le Roux and Stacey, over 50% of underground metal mines all over the world use open stoping

mining systems (Le Roux & Stacey, 2017). Furthermore, the general dilution there exceeds 10%, which leads to instabilities caused by rockfalls and to a reduction in grade of ore and, consequently, to significant economic losses of these mining industries. The authors of the paper provided a new alternative for the conventional ELOS method. Le Roux and Stacey state that the most appropriate hangingwall and sidewall failure prediction system is the new DSSI design criterion (Le Roux & Stacey, 2017). It is based on the ratio of mean stress and volumetric volume, which shows that if the DSSI > 1.0, then there is a failure in tension; in other words, there will be a major sidewall dilution. On the other hand, if DSSI < 1.0, then there will be a failure in compression meaning major hangingwall dilution. Moreover, the authors used a relationship between median stress, volumetric strain, and actual dilution; this relationship was plotted with further regression analysis (R^2). The authors used this relationship between stress, strain, and dilution in order to obtain dilution possibilities from hangingwall and sidewalls. However, the DSSI design criterion should be used in the case of correlation between DSSI and CMS results.

2.4. A brief overview of ELRD

The equivalent linear relaxation depth (ELRD) is another approach for quantifying dilution in stopes. It was developed by Henning and Mitri to estimate potential dilution from a 3D numerical model, where the area of the collapse of the hanging flank is usually identified with the area of tensile stresses (John G Henning & Mitri, 2007). ELRD is based on the ore Dilution Density (DD), which represents probable hanging-wall overbreak and helps to quantify modeled ore dilution from three-dimensional numerical model simulations in the study of dilution in blasthole stoping environment. The term was firstly introduced by Henning in the doctoral dissertation for the same purpose of the denotation of hanging-wall overbreak (John Gordon Henning, 2007). The idea of the DD is that it calculates a volume of potential relaxation that is constrained by a stress contour, most commonly the zero stress contour ($\sigma_3 = 0$) or tensile strength contour of rock mass, where $\sigma_1 = \sigma_3$.

In order to find the dilution density, the following equation is used:

$$DD\ (ELRD) = \frac{Volume\ of\ relaxation\ on\ a\ Stope\ Surface\ (m^3)}{Stope\ Surface\ Area\ (m^2)} \qquad (6)$$

At this point, the term ELRD was introduced in order to distinguish it from the existing ELOS method, which is similar in the way of calculation and use. Furthermore, this

distinguishing can help in the determination of is there is a correlation between dilution and relaxation or not (Wang, 2004). According to Henning and Mitri, the intrinsic characteristic of the definition of ELRD is that it is not constant throughout the studied surface area, allowing for the determination of dilution density at any place in the stope wall (John G Henning & Mitri, 2007). Furthermore, by using one of the stope models (figure 3), we can state that DD is maximum at the center of the modeled stope (DD = r1) and DD is minimum (DD = 0) along the edges of this model.

Moreover, the proposed ELRD model can be modified for results obtained from the cavity monitoring system (CMS). According to the results of overbreak measurement of the stope from CMS outputs, the following equation for DDCMS calculation was obtained:

$$DD_{CMS} = \frac{unplanned\ stope\ volume\ (overbreak\ volume)}{Surface\ area\ of\ exposed\ hangingwall} \qquad (7)$$

The main advantage of the ELRD technique is that the DD is not limited by association with the width of the stopes and the stability number N. During the calculations of DD, the values of the acting stresses on the walls of the stopes, their deflections, and the depth of the zone of the rock mass collapse in the hangingwall of the stopes, are taken into account. The DD value can be calibrated from laser scanning of the camera geometry by CMS systems. Both dilution density values (measured and calculated) can be used together to assess dilution.

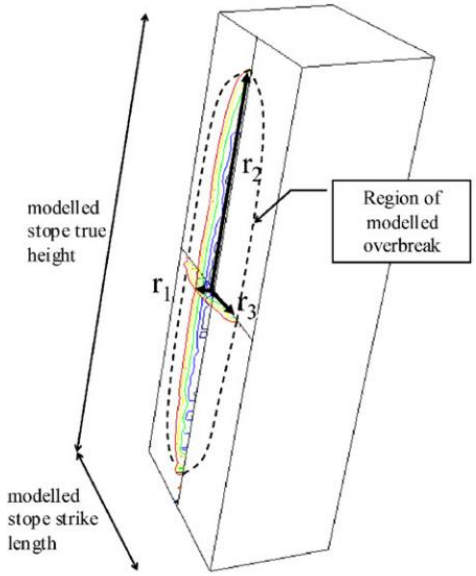

Figure 3. Overbreak envelope in stope hangingwall (Henning and Mitri 2007)

2.5. Other existing studies on Unplanned Dilution Prediction

Numerical Modeling

Apart from conventional graph methods, other attempts were done in order to find more effective and convenient approaches for prediction of unplanned dilution. One of the most popular approaches is using of numerical modeling. In mining engineering, numerical modeling has become one of the most essential and practical tools for the complete examination of ground behavior. In order to construct a cohesive engineered structure, whether on the surface of the rock mass or within the underground rock mass, some type of predictive capability is required. As it was discussed in previous sections, conventional stability graphs are based on analysis of case studies from numerous mines; thus, they are not considered site-specific and their results may not be suitable for specific mine characterization and analysis. Even though stability graphs are used for the design of underground mine infrastructure, a computer model tailored to the unique site circumstances should be used for verification of the similar rock mass behavior (Jing, 2003).

There are two main options in numerical modeling, namely Boundary Element Method (BEM) and Finite Element Method (FEM) or Finite Difference Model (FDM). BEM is used for continuum analysis of stress conditions at excavation boundaries and it assumes that the rock mass is elastic, and often linearly elastic; moreover, it provides for equal treatment of finite and infinite body issues (Brady & Brown, 2006). On the other hand, FEM and FDM is useful for analysis of inelastic rock mass behavior. When compared to these complete domain discretization methods, the fundamental benefit of the BEM is the reduction of the computational model dimension by one, as well as significantly simpler mesh production and hence input data preparation. Due to its direct integral formulation, the BEM is typically more accurate than the FEM and FDM when using the same amount of discretization. Furthermore, unlike the point-wise discontinuous solutions given by the FEM and FDM groups, solutions inside the domain are continuous in BEM (Capes, 2009).

Moreover, BEM is one of the principal modeling approaches of a number of prominent software programs. Boundary element code is used in two and three-dimensional applications such as Examine2D, Examine3D, and Map3D.

Wang, who refined Clark's modeling work in 1998, performed one of the most significant dilution characterizations. Wang used two boundary element technique programs, Examine3D

and Examine2D, to conduct additional modeling research to investigate the link between stope shape, size, stress regime, and a maximum depth of relaxation zone (Wang, 2004). According to his modeling, the stress ratio K has a considerable impact on the HW center's relaxation depth. The greatest relaxation depth increases as the stress ratio K rises. Moreover, the relaxation depth in the center of the stope HW increases, if there is an increase in the hydraulic radius. For the three in-situ stress regimes, the distressed zone depth in the center of the hangingwall or footwall has a linear relationship with the hydraulic radius.

However, there is a limitation of BEM for numerical modeling. This method can be used only with the assumption that the rock mass is homogeneous and has an elastic behavior. For inelastic or plastic rock mass behavior, FEM and FDM are better alternatives (Jing, 2003).

The Rock Engineering System (RES)

The Rock Engineering Systems (RES) technique was first created and implemented by Hudson et al. as a powerful quantitative tool for mining engineering activities (1992). This method is one of the solutions that evaluates all aspects of rock engineering as a system, including all elements that have influenced the situation thus far. In other words, the RES technique evaluates the impact of all existing aspects in rock engineering with the further implementation throughout the entire process, starting from early design considerations and up to construction. The essential element of this strategy is that it mixes several components into a single system, with their effects being taken into consideration in a sensitive way.

The main aim of RES is to create an interaction matrix that identifies the influencing factors as well as their pairwise interactions. To define the linkages between the variables, this interaction matrix must be coded in some fashion. The Expert Semi-Quantitative (ESQ) technique introduced by Hudson (1992) for determining the intensity of interaction necessitates expert knowledge. The completely coupled system performance is established by graph and shown as a Global Interaction Matrix once the basic structure of the problem is specified by the interaction matrix (GIM).

By introducing Dilution Index (DI) into the RES approach, the prediction of dilution levels in the Ridder-Sokolny mine was compiled. The idea was to generate a relationship between Mathew's Stability Number (N') and Dilution Index. According to the results, it was concluded that there is a good correlation (R2 = 0.788), which states that the DI can be used for the prediction of dilution of open stopes in the Ridder-Sokolny mine (M Zhalel, Adoko, & Korigov, 2020)

Machine Learning

As the mining industry is developing, modern investigation approaches are becoming more popular in studying mining aspects. One of the approaches is the utilization of the machine learning method, especially an artificial neural network (ANN). ANN is a computational model with artificial neurons, which have a similar operational concept to brain neural cells. These artificial neurons consist of several parameters, such as input, hidden, output, and numerous basic mathematical elements that make up an ANN's framework. This approach considers the weight of connections between artificial neurons for providing an opportunity to generate a prediction (Yang & Zhang, 1998).

In the case of dilution estimation of underground stopes, the model was used to generate and analyze the correlation between predicted and unplanned dilutions of 160 untrained case studies from Western Australia. According to the results, it was found that there is a good correlation ($R2 = 0.719$) between planned and unplanned dilution values and the authors concluded that the ANN engine can be used as an unplanned dilution predicting tool in underground stopes.

However, the machine learning method has several limitations. The main disadvantage of using the ANN is that models conduct over-fitting, which means that the obtained model is not considered general. In other words, even if the model's fit is perfect during training, it is unable to accurately forecast the output for untrained data. As a result, the cross-validation method provided by Hansen and Salamon should be used to eliminate the over-fitting issue (Hansen & Salamon, 1990).

2.6. Limitations of the stability graph methods and concluding remarks

At this point, the empirical methods of dilution calculations are established as the most convenient way of analysis. However, they have limitations. One of the main limitations is that only the modified stability number and hydraulic radius of the stope are used during the construction of the ELOS empirical graph, but other factors affecting unplanned ore dilution are omitted, which results in errors in the computation findings. Moreover, when the hydraulic radius or modified stability number exceeds the graph's scale range, the application of the ELOS method is severely constrained. Finally, dilution is case-based; thus, using stability graphs, which integrated results from other different case studies makes the dilution results highly generalized and less specific for a certain mine.

Clark and Pakalnis also discussed about the drawbacks of their ELOS dilution graph (1997). According to them, the dilution graph is made up of a small number of case studies (85 case histories), hence this approach is thought to be ambiguous and have a potentially low accuracy. This restriction might be solved by expanding the database of case studies with low-quality rocks and taking large-scale stopes into account. Furthermore, the case studies utilized to create the dilution graph included small-diameter blatsholes (less than 65 mm). Finally, the dilution graph approach does not take into account or recommend stope support.

The recommendation for further analysis is to create an alternative method for calculating dilution based on the specific characteristics of the Ridder-Sokolny mine. Moreover, calculation of dilution is about considering the vast amount of data; thus, the way forward is to integrate empirical methods with machine learning techniques or advanced statistical analysis.

3. UNPLANNED DILUTION ESTIMATION IN RIDDER-SOKOLNY MINE

3.1. Introduction

During a two-month internship on the Ridder-Sokolny mine site, geological and geotechnical data from the departments of the mine were obtained. For this research project, a study created particularly for Ridder-Sokolny mine done by Victor Spirin, who is an SRK Consulting geotechnical engineer, was used. Particularly, geomechanical parameters of the Ridder-Sokolny deposit were considered. Stopes assessed by the Cavity Monitoring System (CMS) provided case histories with real stope dimensions. In order to analyze in-situ stresses surrounding each stope and predict dilution potential owing to relaxation and high induced stresses in the particular mining environment, three-dimensional numerical modeling was used. A thorough database with diverse parameters that may impact the dilution level was built based on the acquired data from reports and numerical modeling findings. The Dilution Index (DI) was established as a means to quantify dilution after a comprehensive investigation of the numerous elements that have an impact on dilution. The Rock Engineering System (RES) was chosen to describe the influential components that cause excessive dilution, evaluate their interactions, compute their weighted coefficients, and produce the Dilution Index, which refers to the possible amount of dilution.

3.2. Background of Ridder-Sokolny mine

3.2.1. General background of mine

The Ridder-Sokolny polymetallic mine is about 3 kilometers from Ridder city in East Kazakhstan (Kazzinc, 2022). Filipp Ridder was the first to discover the Ridder-Sokolny deposit in 1784. Only oxidized ore was extracted there from 1789 until 1861. Production of sulfide ores began in 1885 and continued with only minor interruptions until 1916 when the mine was inundated due to increasing water flow. In the early 1920s, the mine was fully restored (Smirnov, 1978). The main product of the mine is gold with an average grade of 2.0 g/ton with a production rate of 1.6 million tons per year (Yakubov & Adoko, 2020).

The Ridder-Sokolny mine is supervised by Kazakhstani Kazzinc Mining and Metallurgy Company and Canadian Glencore Company. Sublevel caving, shrinkage stoping, upward horizontal slicing with backfilling, 21 sublevel stoping with partial shrinkage applied, and cut-and-fill stoping are some of the mining processes used at Ridder-Sokolny mine, depending on orebody morphology and thickness (Kazzinc, 2022).

The main metals that are hidden in the deposits of this mine are silver, gold, and copper, and their reserves are equal to 2,291 ktons, 9,757 ktons, and 203.1 ktons respectively. In 2020, 1.7 Mt with the grades of 0.2% lead, 0.4% copper, 6 g/tonne of silver, and 2.6 g/tonne of gold were produced. Based on improved LOM and a 2.3Mt annual production throughput, Ridder-Sokolny has a 19-year mine life (Glencore, 2020). Therefore, we can state that Ridder-Sokolny mine is one of the largest providers of raw materials for further manufacturing activities.

3.2.2. Rock mass parameters

The Ridder-Sokolny polymetallic deposit (RSD) is located in the central part of the Leninogorsk ore field between the Northern Thrust and the Obruchev Reverse Fault. The rock mass is composed of volcanic-sedimentary rocks of the Devonian age, which are divided into suites (from bottom to top): Leninogorskaya, Kryukovskaya, Ilyinskaya, and Sokolnaya. The main volume of industrial mineralization is concentrated in the rocks of the Kryukovskaya suite, which conformably overlies the Leninogorskaya suite and is overlain by the rocks of the Ilyinskaya and Sokolnaya suites. Here, the Kryukovskaya suite is a 500-540 m thick sequence of calcareous, clayey, siliceous siltstones with interlayers of sandstones, gravelstones, and porphyrite breccias. The rock mass situation is represented on Figure 4.

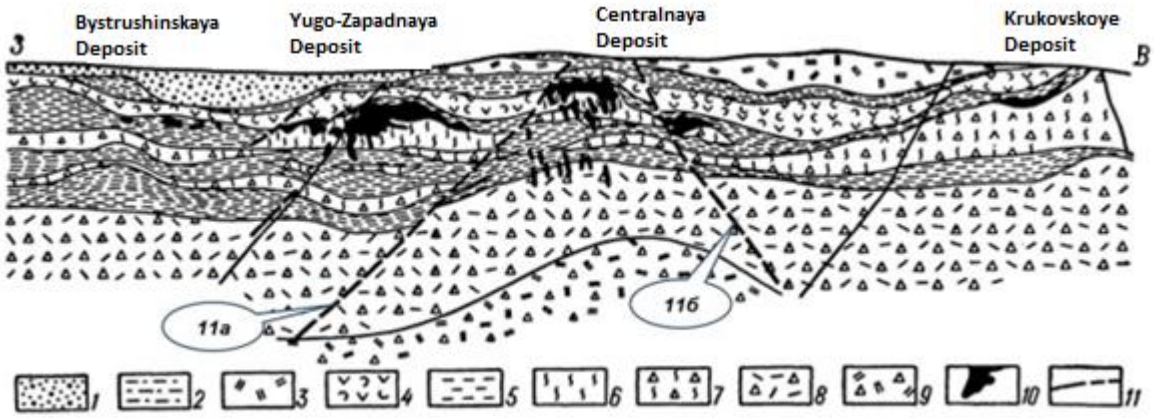

Figure 4. Schematic cross-section of the Ridder-Sokolny deposit

The general structure of the ore deposits can be characterized as "jellyfish" - a combination of gently dipping and steeply dipping ore bodies. The gently sloping deposits of the upper horizon of mineralization had a wide areal development throughout the deposit. By now, almost all of them have been worked out. Only sections of deposits on the flanks of the deposit remained undeveloped. The total number of ore bodies is more than 10,000. The vast majority are dominated by ore bodies with a small thickness and extent, both in dip direction and in dip angle. Parameters of ore deposits based on the results of the calculation of reserves performed by LLP "Geoincenter" in 2001 are presented in the following table (see **Table 1**).

Table 1. Characterization of Ridder-Sokolny Orebodies

Deposit name	Reserve percentage, %		Dimensions of orebodies, %			
	Flat	Dipping	Along strike		Thickness	
			< 100 m	> 100 m	< 10 m	> 10 m
Zavodskaya	50	50	94	6	99	1
Riderskaya	9	91	97	3	100	0
Vtoraya Riderskaya	38	62	94	6	100	0
Centralnaya	3	97	95	5	99	1
Pobeda	23	77	95	5	99	1
Perspektivnaya	50	50	92	8	100	0
Belkina	79	21	89	11	100	0
Pervaya Yugo-Zapadnaya	19	81	93	7	99	1
Vtoraya Yugo-Zapadnaya	7	93	96	4	100	0
Tretya Yugo-Zapadnaya	4	94	94	6	88	12
Bystrushinskaya	6	94	95	5	100	0

Here, we can see that there is an almost equal amount of flat and dipping ore reserves in Ridde-Sokolny deposits. Moreover, the largest proportion of orebodies are shorter than 100 m in length and thickness is mostly less than 10 m.

Furthermore, there are 14 main rock types in Ridder-Sokolny deposit. By testing 20 core samples on a Uniaxial Compressive Strength (UCS) testing machine, rock types prone to rock bursts were identified. Hard, strong rocks with elastic deformation to failure and brittle fracture character are prone to rock bumps. The elastic modulus E and the decay modulus M are measured by testing the samples on UCS machines. When E/M is less than one, the rock is regarded as prone to rock bumps; when E/M is greater than one, the rock is not considered prone to rock bumps (Makarov, 2013).

According to the results, tests have established that in microquartzites, agglomerate tuffites, quartz felsite porphyries, and in tuffs, the E / M value is 0.2-0.6, therefore these rocks are prone to brittle fracture and can be classified as potentially shock-hazardous. Thus, we can see that 4 rock types out of 14 are prone to rock bursts (Makarov, 2013).

Furthermore, the main deposit, where the most mining activities are performed (Kryokovskoye deposit) consists of ten faults, where Severniy Nadvig fault is the largest of them. Finally, as it

was mention, there are 14 rock types that are divided into six domains for simpler analysis (see **Table 2**).

Table 2. Rock Mass Parameters and Ratings

Geotechnical domains	RMR (B89)	GSI (JCond89)	GSI (Jr, Ja)	Q'
2+3+4+5+19	58	58	65	16
9+10	68	64	71	15
11	54	43	59	9
12	60	66	73	17
13	60	70	77	19
15+17	68	72	79	20

After the mapping of discontinuities and thorough analysis of them, the author was able to characterize the rock mass quality by using three main rock mass classification methods. First of all, it was concluded that there are four major systems of discontinuities. According to rock mass rating calculations, each of the six domains has its rock mass rating (RMR), Q-system, and GSI values. The values can be observed in Table 2.

3.2.3. Mining method

Sublevel caving, cut-and-fill stoping, sublevel stoping with partial shrinkage applied, shrinkage stoping, upward horizontal slicing with backfilling, and sublevel caving are some of the mining processes used at Ridder-Sokolny mine, depending on orebody morphology and thickness. At this point, the most common mining method is an underground open-stoping method. The ore is collected from massive non-entry excavations utilizing automated equipment in an open stope mining process. Workers are not permitted to enter open stopes due to the risk of waste rock failure due to stope surface instability (MEIIRKHAN ZHALEL, 2019).

3.2.4. Description of the unplanned dilution data

The challenge that Ridder-Sokolny mine is facing for a long period is the ore dilution. According to the geotechnical report produced by SRK Consulting, traditional dilution calculation methods (ELOS and ELRD) were used to calculate both planned and unplanned ore dilution levels (Biryuchev, 2018). Based on these findings, the authors hypothesized that when the stopes are in an unstable state, unanticipated dilution can raise the targeted amount of dilution by 2.1 percent, and in collapsed stopes, it can rise by an average of 4.3 percent.

However, the true dilution levels in some stopes are around 1000 percent higher than the anticipated values. Some data about dilution by stopes can be seen in **Table 3**.

Table 3. Ore Dilution Calculations from 2013 to 2017 (Biryuchev, 2018).

Deposit	Name of the mining unit	Ore dilution			
		Planned dilution		Actual dilution	
		%	Tons	%	Tons
Bystrushenskaya	Stope 36	19.1	6522	13.1	4473
Bystrushenskaya	Block 95 Stope 8	3.8	306	53.5	4311
Bystrushenskaya	Block 95 Stope 10	6.4	682	56.1	2341
North wing of Bystrushinskaya	Block 94 Stope 5	21	82.3	3	118
Vtoraya Yugo-Zapadnaya	Block 79 Stope 1	13.5	2433	14	2549
Vtoraya Yugo-Zapadnaya	Block 79 Stope 5	10.2	4594	11.4	5145
Vtoraya Yugo-Zapadnaya	Panel 15	23.9	18401	30.6	22237
Pobeda	Block 36/3	23.3	17273	36.8	27300
Pobeda	Panel 150	21.1	11444	24.3	13117

According to the table, we can see that, for example, the projected dilution of the Bystrushinskaya deposit, block 95, stope 8, is 3.8 percent; however, the true dilution is 53.5 percent. More than half of the stopes evaluated have comparable situations (Biryuchev, 2018). Moreover, the challenge of high unplanned dilution is common not in every stope, panel, or block. For example, Block 94, Stope 5 shows that the actual dilution is lower by 18% (21% and 3%).

3.2.5. Dilution graphs

The stability of the excavation units was examined using the Matthews stability graph method, and the findings were compared to the current situation. As a consequence, a rock stability diagram of the Ridder-Sokolny stopes was created. The diagram is based on historical and current data on the state of goaf regions, and a realistic database has been built to assess rock collapse situations on the Ridder mine. It consisted of 160 excavation units, 70 of which are stable (Stable), 31 of which are unstable (Unstable), and 59 of which had fully collapsed rock masses (Caved). The diagram can be seen in ***Figure 5***.

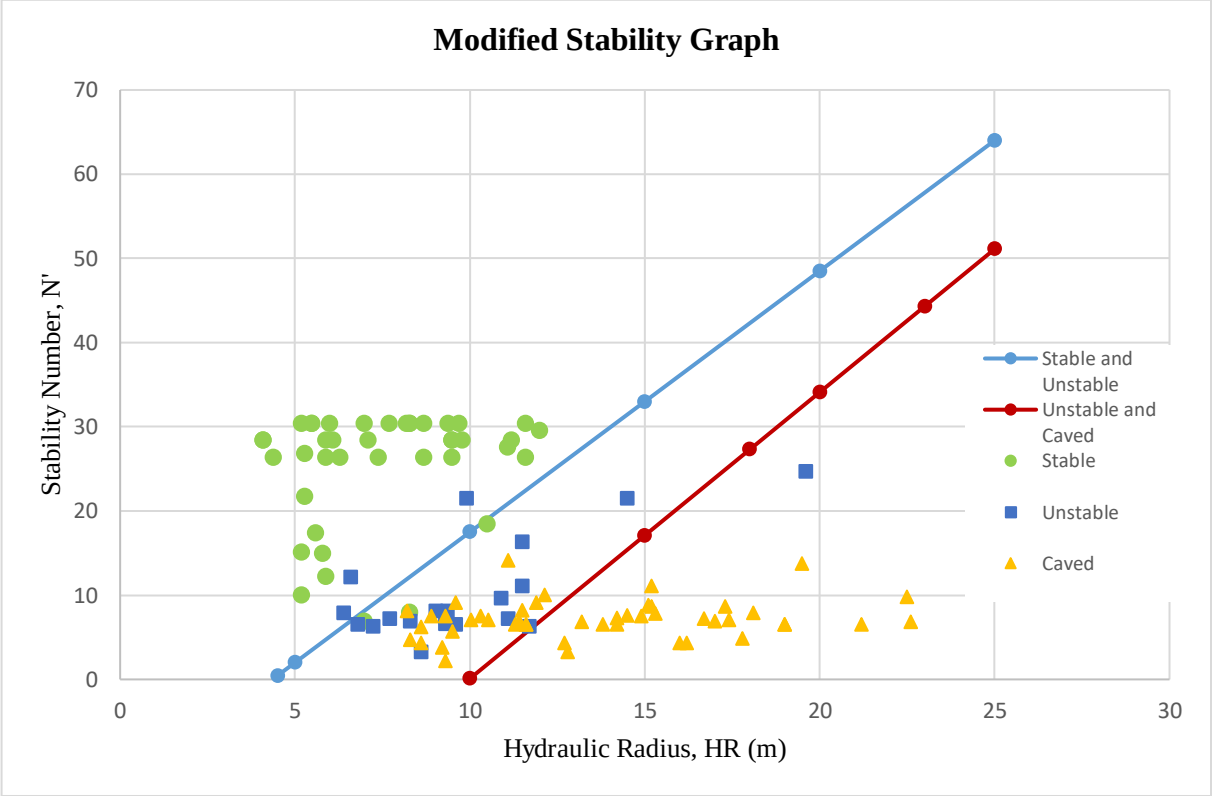

Figure 5. Stability Graph used in Ridder-Sokolny mine

In Figure 5, the area of stable states of stopes is to the left and above the green line, the area of collapsed states of stopes is below and to the right of the red line. Furthermore, according to the created stability graph, it is possible to design the mining of ore bodies on the Ridder mine, ensuring the stability of the stopes, by setting the appropriate hydraulic radius values.

Furthermore, the accuracy of the modified stability graph was estimated by comparing the predicted stability state by graph and the actual stability of the stopes (see ***Table 4***).

Table 4. Modified Stability Graph accuracy

		Predicted from Graph		
Actual State		**Stable**	**Unstable**	**Caved**
	Stable	38	3	0
	Unstable	3	15	1
	Caved	0	21	26

Here, the accuracy of the graph was estimated as 74%. It shows moderate accuracy, but it is still not accurate enough.

ELOS dilution estimation by the rocks of the hangingwall of the stopes at the Ridder mine was produced based on the data gathered. This evaluation was carried out by comparing empirical values (ELOS = 0.5, 1.0, 2.0 m) with real dilution data for various stopes stability states (Stable, Unstable, Caved). ELOS dilution graph is presented in ***Figure 6.***

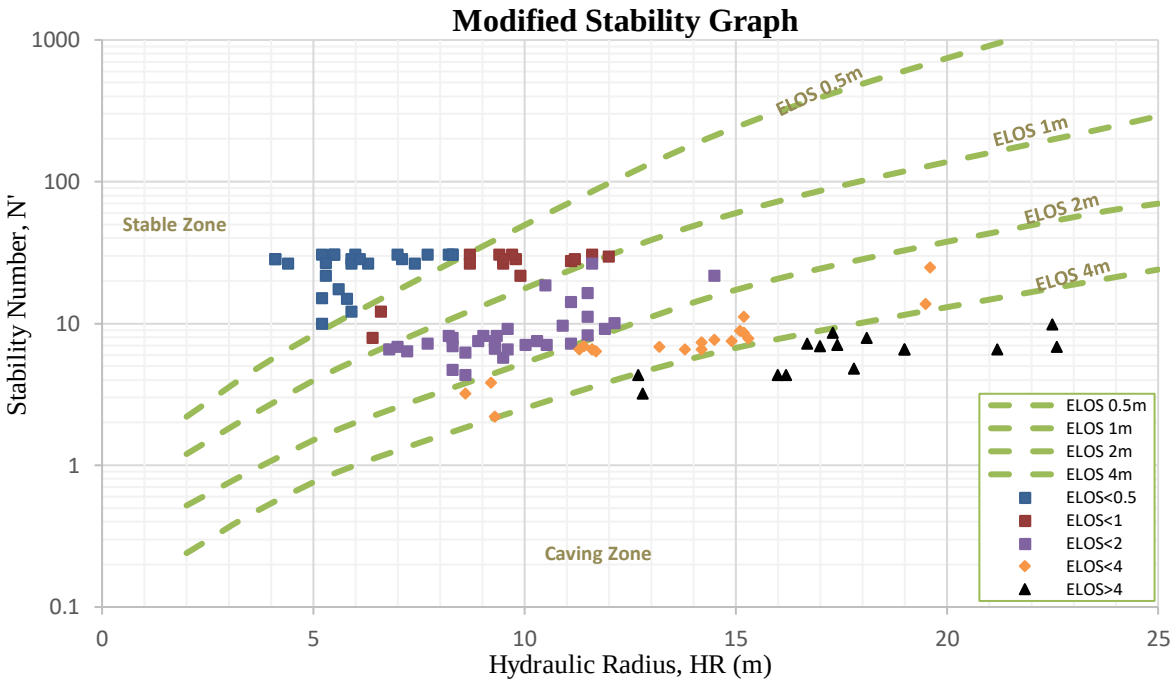

Figure 6. ELOS Dilution Graph

The average levels of acceptable unplanned dilution values of stopes in Ridder-Sokolny mine estimated by specialists of SRK Consulting is approximately 20%. The accuracy of the ELOS stability graph was estimated by comparing the predicted ELOS value by graph and the actual ELOS of the stopes (see ***Table 5***).

Table 5. ELOS Stability Graph accuracy

		Predicted from Graph				
Actual State		**ELOS < 0.5**	**ELOS < 1**	**ELOS < 2**	**ELOS < 4**	**ELOS > 4**
	ELOS < 0.5	9	5	14	10	11
	ELOS < 1	15	9	16	10	4
	ELOS < 2	1	1	2	0	0
	ELOS < 4	0	0	0	0	0
	ELOS > 4	0	0	0	0	0

Finally, data on 107 case studies of open stopes were collected for further analysis of ELOS stability graph accuracy. Planned dilutions were compared with actual dilution results obtained from CMS records.

3.3. Multinomial Regression

3.3.1. Introduction

First of all, there exist various methods for estimation and analysis of the stability of underground stopes, such as numerical modeling, back analysis of in-situ measurements of stope performance, analytical methods, and empirical graphs. Numerical modeling is established as an effective way for predicting the mechanical reaction of underground stopes on excavation activities; however, it is challenging to get good rock mass data as variables that should be considered as an input. In this case, it is more convenient to use empirical graph methods for stability analysis of stopes even though the results can be subjective as the stability graph zones are generated manually by the user (M Zhalel et al., 2020).

3.3.2. Dataset generation

The database created by SRK Consulting's experts was utilized in this investigation. The data consists of two main parameters of stope stability prediction, namely Stability Number (N) and Hydraulic Radius (HR), and the related dilution values. The database consists of 107 case study stopes, where they were divided into three dilution classes (major, moderate, and minor) and the dilution ranges for each of the class can be observed in the following table (see ***Table 6***).

Table 6. Dilution Classes

Dilution Class	**Dilution ranges**
Major	Dilution > 25%
Moderate	15% < Dilution ≤ 25%
Minor	Dilution ≤ 15%

The frequency of each dilution class in dataset is presented in the following histogram (see ***Figure 7***).

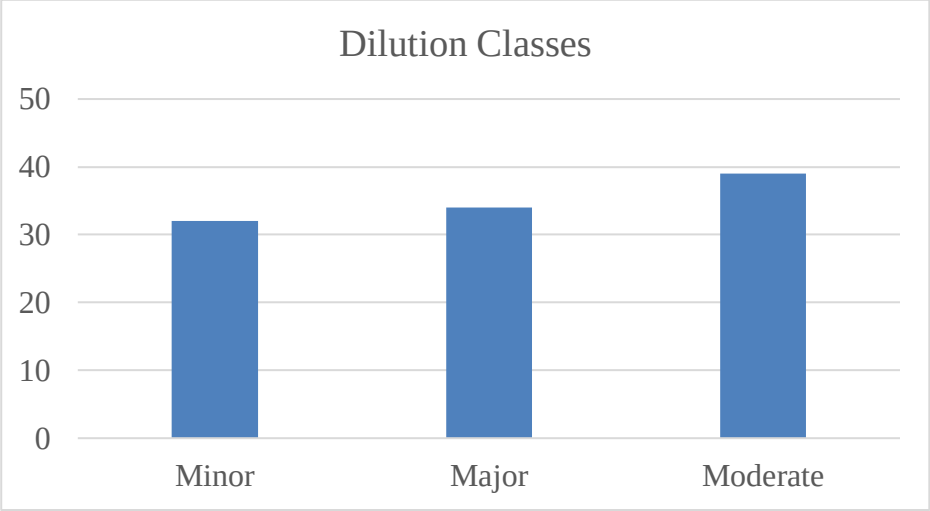

Figure 7. Dilution classes

According to the classification of the unplanned dilution, ELOS Stability Graph with these data points was produced (see ***Figure 8***).

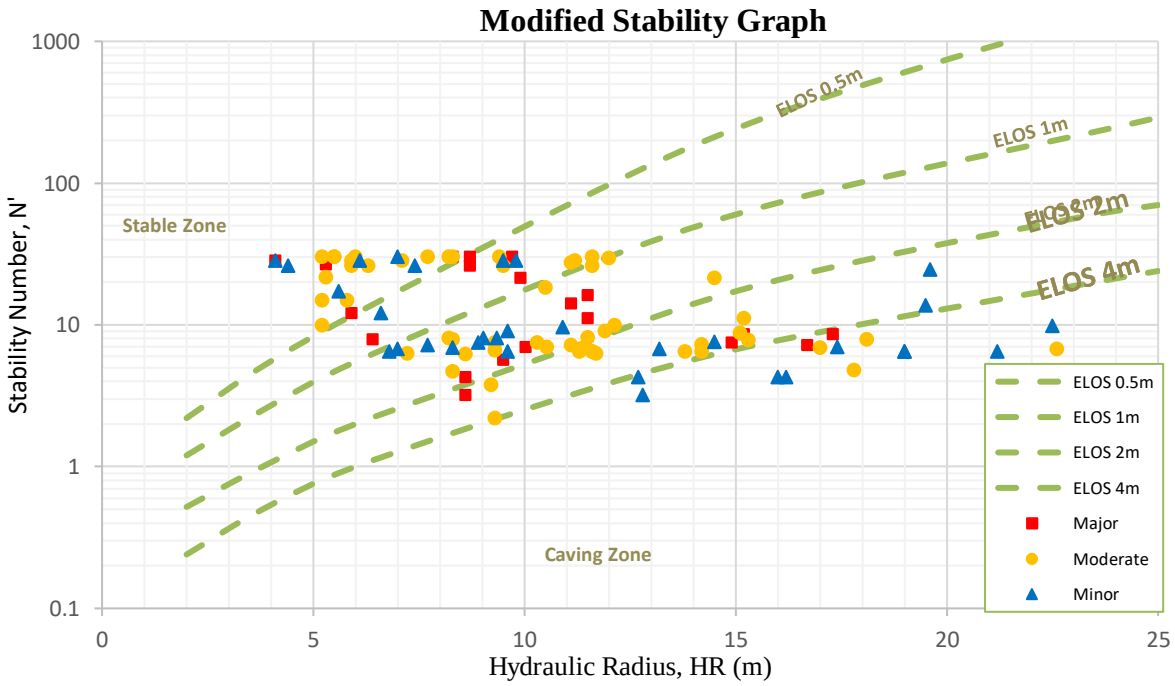

Figure 8. ELOS Graph with Dilution Classes

In ***Figure 8***, it can be seen that the dilution classes are represented in wrong ELOS zones. For example, some stopes with actual major dilution are located in stable zone with ELOS ≤ 0.5 m; however, ELOS ≤ 5 means that the stope should have low dilution.

3.3.3. The Multinomial Logistics Regression (MLR)

When the response variable has more than two possible outcomes, multinomial logistic regression (MLR) is used instead of a simple binary logistic regression. Thus, the MLR is used for the estimation of the possibility of several probable results. In the case of Ridder-Sokolny Mine, we are dealing with three conceivable outcomes of stope dilution, namely major, moderate, and minor. The main purpose of the MLR is to model the link between independent variables and the stope dilution results; consequently, the MLR may be used to reliably forecast new data points given known independent variables. If we consider the following parameters, we can represent the MLR model as a series of binary logistic regressions with the Kth (see Equation 9):

- *N* data points → $i = 1, 2, 3, 4, \ldots, n$
- *M* independent variables → $\mathbf{X_i} = (x_{i1}, x_{i2}, x_{i3}, x_{i4}, \ldots, x_{im})$
- Y_i multinomial outcomes → $K = 1, 2, 3, 4, \ldots, k$

$$P(Y_i = k - 1|X_i) = \frac{e^{\boldsymbol{\beta}_{k-1}\boldsymbol{X}_i}}{1+\sum_{k=1}^{K-1} e^{\boldsymbol{\beta}_k \boldsymbol{X}_i}} \qquad (8)$$

- $\boldsymbol{\beta}_k \mathbf{X}_i = \beta_{0,k} + \beta_{1,k} x_{1i} + \beta_{2,k} x_{2i} + \beta_{3,k} x_{3i} + \ldots + \beta_{m,k} x_{mi}$
- $\boldsymbol{\beta}_k = (\beta_{0,k}, \beta_{1,k}, \beta_{2,k}, \beta_{3,k}, \ldots \beta_{m,k})$ → the regression coefficient with
    - *m*th dependent variable
    - *k*th outcome

There are several probabilities for each of the three potential outcomes (major, moderate, and minor) depending on whether the dependent variable Y is coded as 0, 1, or 2 and whether Y=0 is used as a pivot or reference. The probabilities for these outcomes can be presented as:

$$P(Y = 0|\boldsymbol{x}) = \frac{1}{1+e^{g_1(x)}+e^{g_2(x)}} \qquad (9)$$

$$P(Y = 1|\boldsymbol{x}) = \frac{e^{g_1(x)}}{1+e^{g_1(x)}+e^{g_2(x)}} \qquad (10)$$

$$P(Y = 2|\boldsymbol{x}) = \frac{e^{g_2(x)}}{1+e^{g_1(x)}+e^{g_2(x)}} \qquad (11)$$

Here:

$$g_1(\boldsymbol{x}) = \ln\left[\frac{P(Y=1|\boldsymbol{x})}{P(Y=0|\boldsymbol{x})}\right] = \beta_{10} + \beta_{11}x_1 + \beta_{12}x_2 + \ldots + \beta_{1p}x_1 = \boldsymbol{x}'\beta_1 \qquad (12)$$

$$g_2(\boldsymbol{x}) = \ln\left[\frac{P(Y=2|\boldsymbol{x})}{P(Y=0|\boldsymbol{x})}\right] = \beta_{20} + \beta_{21}x_1 + \beta_{22}x_2 + \ldots + \beta_{2p}x_1 = \boldsymbol{x}'\beta_2 \qquad (13)$$

The dilution values were distributed into the classes according to the dilution value criteria (see ***Table 7***).

Table 7. Dilution classes

Dilution Class	**Dilution ranges**
Major	Dilution > 25%
Moderate	15% < Dilution ≤ 25%
Minor	Dilution ≤ 15%

Furthermore, another scenario was considered and analyzed in an attempt to find more convenient dilution ranges for stope dilution predication. In this case, the dependent variable Y is coded as 0, 1, where Y = 0 is a possibility of a minor dilution outcome and Y = 1 is a probability of a major dilution outcome. As in the previous scenario, Y = 0 is used as a reference point. The probabilities for these outcomes can be presented as:

$$P(Y=0|\boldsymbol{x}) = \frac{1}{1+e^{g_1(x)}} \qquad (14)$$

$$P(Y=1|\boldsymbol{x}) = \frac{e^{g_1(x)}}{1+e^{g_1(x)}} \qquad (15)$$

Here:

$$g_1(\boldsymbol{x}) = \ln\left[\frac{P(Y=1|\boldsymbol{x})}{P(Y=0|\boldsymbol{x})}\right] = \beta_{10} + \beta_{11}x_1 + \beta_{12}x_2 + \ldots + \beta_{1p}x_1 = \boldsymbol{x}'\beta_1 \qquad (16)$$

The distribution of dilution values is presented in the following table (see ***Table 8***).

Table 8. Dilution classes

Dilution Class	**Dilution ranges**
Major	Dilution > 20%
Minor	Dilution ≤ 20%

4. RESULTS

The multinomial logistic regression model was established by defining the open stope dilution criteria as 0, 1 and 2 for three possible outcomes, namely moderate, major and minor dilutions. For the production of the MLR model, IBM SPSS Statistics software was used. The software provided statistical summary results by considering the parameter estimations and these data is presented in the following table (see ***Table 9***). The open stope dilution classification is the dependent variable, whereas N and HR are independent factors. Moderate dilution class was chosen as the reference point.

Table 9. Estimated regression parameters (Scenario 1)

Parameter Estimates		
Dilution		**B**
Major	Intercept	.733
	HR	-.037
	N	-.021
Minor	Intercept	-.054
	HR	.033
	N	-.031

- B – Regression coefficients

Here is how the logistic regression equations were used:

$$P(Modearte) = \frac{1}{1+e^{0.733-0.037*HR-0.21*N}+e^{-0.054+0.033*HR-0.031*N}} \quad (17)$$

$$P(Major) = \frac{e^{0.733-0.037*HR-0.21*N}}{1+e^{0.733-0.037*HR-0.21*N}+e^{-0.054+0.033*HR-0.031*N}} \quad (18)$$

$$P(Minor) = \frac{e^{-0.054+0.033*HR-0.031*N}}{1+e^{0.733-0.037*HR-0.21*N}+e^{-0.054+0.033*HR-0.031*N}} \quad (19)$$

Furthermore, it is necessary to evaluate the performance of the MLR analysis. The SPSS software provided the accuracy of prediction of underground stope dilution classification, which is presented in the following table (see ***Table 10***).

Table 10. The accuracy of the MLR model for the First Scenario

Classification prediction				
	Prediction			
Observed	Major	Minor	Moderate	Percent Correct
Major	19	5	14	50.00%
Minor	13	12	7	37.50%
Moderate	13	9	15	40.50%
Overall percentage	42.10%	24.30%	33.60%	43.00%

Furthermore, another possible scenario was analyzed with two dilution classes, namely minor and major dilutions. Here, minor dilution was chosen as the reference point. Based on parameter estimates, the program generated statistically significant findings, which are shown in the table below (see ***Table 11***).

Table 11. Estimated regression parameter (Scenario 2)

Parameter Estimates		
Dilution		**B**
Major	Intercept	1.188
	HR	-.109
	N	.010

Here are how the logistic regression equations were used for this scenario:

$$P(Minor) = \frac{1}{1+e^{1.188-0.109*HR+0.01*N}} \qquad (20)$$

$$P(Major) = \frac{e^{1.188-0.109*HR+0.01*N}}{1+e^{1.188-0.109*HR+0.01*N}} \qquad (21)$$

The SPSS software also provided the accuracy of prediction of underground stope dilution classification, which is presented in the following table (see ***Table 12***).

Table 12. The accuracy of the MLR model for the second scenario

Classification prediction			
	Prediction		
Observed	Major	Minor	Percent Correct
Major	46	12	79.3%
Minor	28	21	42.9%
Overall percentage	69.2%	30.8%	62.6%

Dilution values were compared to predicted probability of major, moderate and minor dilution classes for each case study stope. Appendix B contains the findings.

Furthermore, ***Figure 9*** shows a two-dimensional color-coded graph representing the probability of the occurrence of major dilution.

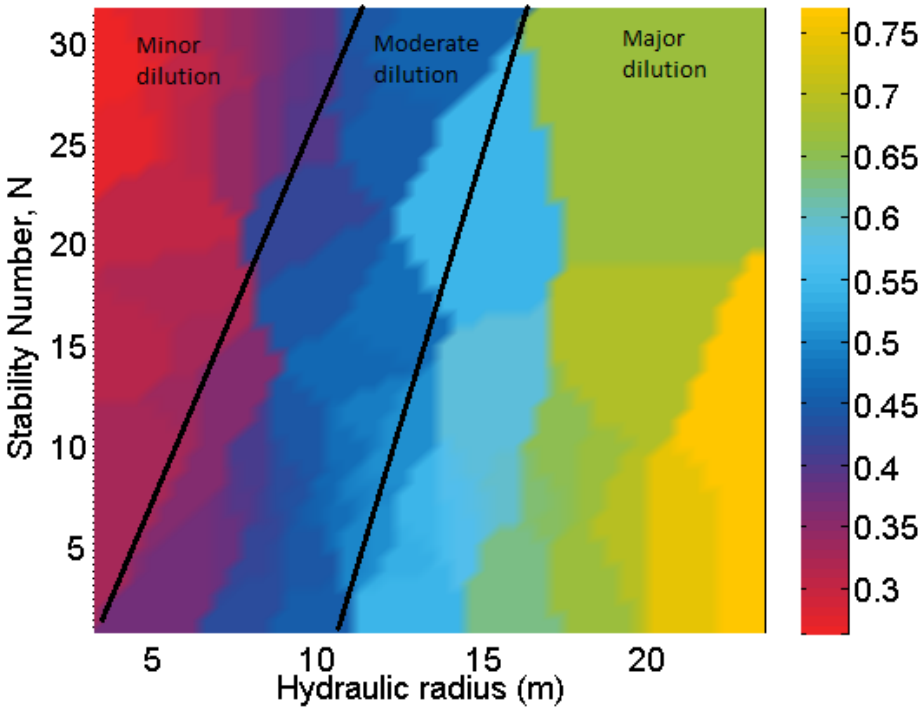

Figure 9. Probabilistic Map for Major Dilution

In the ***Figure 9***, probabilities with a certain color code are used to depict dilution zones. Data points that fall inside the red zone (probability < 0.4) have a likelihood of experiencing minor dilution. Points that are located in the blue zone (probability < 0.6 and > 0.4) have probability

of experiencing moderate dilution. And finally data points in the green zone (probability > 0.6) show probability of experiencing major dilution. For example, if we consider an open stope with N' value of 20 and HR value of 5, then there is a high probability of stope having major dilution.

5. DISCUSSION

First of all, a complete database of planned and unplanned dilution based on accessible data of hydraulic radius and modified stability numbers was generated. It helped to observe that 87 out of 107 case studies of stopes of Ridder-Sokolny mine have different planned dilution and actual dilution values.

It was crucial to collect data about the planned dilution calculated through ELOS method and further actual dilution results from CMS measurement. According to data provided by geotechnical department of the Ridder-Sokolny mine and reports done by SRK Consulting, 107 case studies were analyzed in this research. The data wasn't always in the right format, and there was a lot of information that was missing. For example, ELOS data for some of the stopes was not specified by the department; thus, it was necessary to calculate them through ELOS stability graph (see ***Figure 6.*** ELOS Dilution Graph). Table 1 in Appendix A represents the whole data set of factors that were used in the analysis.

By considering data provided in Appendix A, it was necessary to calculate ELOS of stopes and classify them into 5 classes (see ***Table 13***). Furthermore, ELOS values were transformed into planned dilution measures through the following equation (Papaioanou & Suorineni, 2016):

$$Dilution = \frac{ELOS}{Orebody\ Width} * 100\% \qquad (22)$$

Table 13. ELOS Classes

ELOS Classes	Range
1	ELOS < 0.5
2	0.5 ≤ ELOS < 1
3	1 ≤ ELOS < 2
4	2 ≤ ELOS < 4
5	ELOS ≥ 4

Next, it was crucial to compare actual dilution results and their ELOS classes with planned dilution ELOS values (see Table 2 Appendix A). It was concluded that the planned dilution ELOS values and actual dilution ELOS values differ dramatically. To be more precise, out of 107 case studies, 20 of them showed the same planned and actual ELOS values; however, 87 of them showed different results. This analysis confirms that the conventional ELOS dilution graph is an unreliable way to calculate dilution of stopes and it shows that the Ridder-Sokolny mine requires more convenient approach for dilution calculation. The reason for the poor performance of the ELOS stability graph for dilution estimation is that this approach does not consider blasting parameters such as diameter and length of blasts, blast hole layout, and the number of blasts. Moreover, irregular shapes of orebodies are not considered in the ELOS method, as well as it does not differentiate between narrow and massive orebodies, which can affect the accuracy of dilution estimation.

Furthermore, the Multinomial Logistic Regression model was used to calculate the probability of stope stability. Dilution levels at Ridder-Sokolny mine were properly estimated using this method.

In the case of the first scenario with 3 dilution classes (major, moderate, and minor), the overall percentage of correct predictions is equal to 43% and it indicates moderate accuracy. However, the second scenario with 2 dilution classes (major and minor) represents the overall percentage of correct predictions equal to 62.6% and it indicates good accuracy. It should be noted that this scenario shows higher accuracy than the case with three dilution classes.

The problem of insufficient accuracy of dilution predictions is probably generated due to the lack of an appropriate dataset. Reports on geotechnical and geological conditions of the Ridder-Sokolny mine provided by SRK Consulting did not contain dilution data on every stope; as a result, the number of case studies (107 stopes) was not enough for a more accurate multinomial logistic regression analysis. Moreover, the dimensions of some stopes were too large or too small. For example, there is a stope (Perspektivnaya deposit, Block 21) that has a width of 140 m, a height of 17 m, and a length of 35 m. A width of 140 m for one stope could be estimated inaccurately because such a width value will probably lead to severe instabilities. The mine administration probably would not allow such dimensions of the stope, as the rock mass strength has only moderate stability conditions.

Moreover, there could be some deviations from the accurate calculation of actual stope dilution and stope dimensions with corresponding HR and N parameters. This challenge could also lead to inaccuracy in the multinomial logistic regression analysis.

Furthermore, the probability map was generated for major dilution possibility. Open stope stability estimation was viewed in a new light through the use of the multinomial logistic regression probability plot. Percentages of confidence may be calculated for open stope stability interpretation using this approach. The probability map included certain Ridder-Sokolny mine dilution numbers. For example, points (open stopes) that are located in the green zone will probably suffer major dilution. On the other hand, data points that are located in the red zone will probably have minor dilution (see ***Figure 9***).

The probability map generated by multinomial regression analysis can be used as a replacement for the conventionally utilized Mathew's Stability Graph. As a result of this strategy, classic modified stability graph misinterpretations are no longer an issue. The modified stability graph predicts that a given stope will be stable, unstable or caved, which is not always the case in actual mining environments.

6. CONCLUSION AND RECOMMENDATIONS

One of the most serious challenges in most mining operations is unplanned open stope dilution. This problem forced to conduct research to assess the impact of rock mass characteristics and in-situ stress regime on stope design and performance at Ridder-Sokolny Mine in terms of instability and dilution. Several achievements were accomplished by this research project.

Analysis of ELOS stability graph accuracy was carried out using data from 107 open stopes of Ridder-Sokolny mine. The actual dilution results acquired from CMS data were compared to the planned dilutions. It resulted that the conventional ELOS stability graph for unplanned dilution estimation is a poor approach for the prediction of dilution at the Ridder-Sokolny mine, as 87 stope dilution cases out of 107 have different planned and actual dilution values.

Furthermore, using the Multinomial Logistic Regression (MLR) model, a novel probabilistic approach was created that provided the probability of unplanned dilution of open stopes. This method helped to accurately estimate dilution levels in the Ridder-Sokolny mine.

The use of the MLR method generated a probabilistic map that showed that this map can be utilized as an alternative to conventional stability graph approaches, such as Mathew's Stability Graph and ELOS Stability Graph. It shows the stability status as a percentage, which is a more

precise and appropriate approach to estimate and predict stability and possible dilution of underground open stopes.

Moreover, this topic needs further research and investigation for a better understanding and prediction of planned and unplanned dilution results. First of all, the amount of data that was used in this work is limited and based only on reports and papers written on Ridder-Sokolny mine. Therefore, there should be done more site works and studies by researchers on the actual and up-to-date state of dilution and stope stability. It will help to upgrade the quality and size of the geotechnical database.

The impact of blasting also was not taken into account in this investigation. Overbreak and underbreak can be influenced by a variety of blasting factors including powder factor, load, spacing, and drillhole deviations. Undercutting and exposure duration should also be carefully considered.

7. REFERENCES

Bazarbay, B., & Adoko, A. (2021). *Development of a knowledge-based system for assessing unplanned dilution in open stopes.* Paper presented at the IOP Conference Series: Earth and Environmental Science.

Biryuchev, I., Spirin, V., Makarov, A., Batalov, A., Sultanov, L., Bondarenko, R. . (2018). *Assessment of the geomechanical state of the rock mass at the Ridder-Sokolny mine [Оценка геомеханического состояния горного массива на Риддер-Сокольном руднике]* Retrieved from

Brady, B. H., & Brown, E. T. (2006). *Rock mechanics: for underground mining*: Springer science & business media.

Capes, G. W. (2009). *Open stope hangingwall design based on general and detailed data collection in rock masses with unfavourable hangingwall conditions* (Vol. 71).

Clark, L., & Pakalnis, R. (1997). *An empirical design approach for estimating unplanned dilution from open stope hangingwalls and footwalls.* Paper presented at the Presentation at 99th Canadian Institute of Mining annual conference, Vancouver, BC.

Clark, L. M. (1998). *Minimizing dilution in open stope mining with a focus on stope design and narrow vein longhole blasting.* University of British Columbia,

Diakité, O. (1998). Ore dilution in sublevel stoping.

Feng, X., Wang, L., Bi, L., Jia, M., & Gong, Y. (2008). Collapsibility of orebody based on Mathews stability graph approach. *Chin. J. Geotech. Eng, 30*(4), 600-604.

Glencore. (2020). *Resources and Reserves*. Retrieved from https://www.glencore.com/dam/jcr:3c05a365-e6ae-4c1a-9439-960249a42e35/GLEN_2020_Resources_reserves_report.pdf

Hansen, L. K., & Salamon, P. (1990). Neural network ensembles. *IEEE transactions on pattern analysis and machine intelligence, 12*(10), 993-1001.

Henning, J. G. (2007). Evaluation of long-hole mine design influences on unplanned ore dilution.

Henning, J. G., & Mitri, H. S. (2007). Numerical modelling of ore dilution in blasthole stoping. *International Journal of Rock Mechanics and Mining Sciences, 44*(5), 692-703.

Henning, J. G., & Mitri, H. S. (2008). Assessment and control of ore dilution in long hole mining: case studies. *Geotechnical and Geological Engineering, 26*(4), 349-366.

Jang, H., Topal, E., & Kawamura, Y. (2015). Unplanned dilution and ore loss prediction in longhole stoping mines via multiple regression and artificial neural network analyses. *Journal of the Southern African Institute of Mining and Metallurgy, 115*(5), 449-456.

Jing, L. (2003). A review of techniques, advances and outstanding issues in numerical modelling for rock mechanics and rock engineering. *International Journal of Rock Mechanics and Mining Sciences, 40*(3), 283-353.

Kazzinc. (2022). Ridder-Sokolny Mine Retrieved from https://www.kazzinc.com/eng/o-proizvodstve/predpriyatiya/ridder-sokolnyj-rudnik

Le Roux, P., & Stacey, T. (2017). Value creation in a mine operating with open stoping mining methods. *Journal of the Southern African Institute of Mining and Metallurgy, 117*(2), 133-142.

Makarov, A. (2013). *Development of recommendations for the reactivation of ore reserves from safety pillars for protected surface and underground facilities of the RSR. [Разработка рекомендаций по расконсервации запасов руды из предохранительных целиков под охраняемые поверхностные и подземные объекты РСР]*. Retrieved from

Mawdesley, C., Trueman, R., & Whiten, W. (2001). Extending the Mathews stability graph for open–stope design. *Mining Technology, 110*(1), 27-39.

Pakalnis, R. T. (1986). *Empirical stope design at the Ruttan Mine, Sherritt Gordon Mines Ltd.* University of British Columbia,

Papaioanou, A., & Suorineni, F. (2016). Development of a generalised dilution-based stability graph for open stope design. *Mining Technology, 125*(2), 121-128.

Potvin, Y. (1988). *Empirical open stope design in Canada.* University of British Columbia,

Smirnov, V. (1978). Ore Deposits of the USSR (in 3 volumes). *Nedra, Moscow, 3*.

Stewart, P., & Trueman, R. (2001). *The Extended Mathews Stability Graph: Quantifying case history requirements and site-specific effects*.

Suorineni, F. T. (2010). The stability graph after three decades in use: experiences and the way forward. *International journal of mining, Reclamation and Environment, 24*(4), 307-339.

Villaescusa, E. (1998). Geotechnical design for dilution control in underground mining. *Mine Planning and Equipment Selection*, 141-149.

Wang, J. (2004). Influence of stress, undercutting, blasting and time on open stope stability and dilution.

Yakubov, K., & Adoko, A. (2020). *A reliability analysis of underground mine drift support in Ridder-Sokolny mine, Kazakhstan.* Paper presented at the ISRM International Symposium-EUROCK 2020.

Yang, Y.-j., & Zhang, Q. (1998). The application of neural networks to rock engineering systems (RES). *International Journal of Rock Mechanics and Mining Sciences, 35*(6), 727-745.

ZHALEL, M. (2019). DILUTION ASSESSMENT AT RIDDER-SOKOLNY MINE.

Zhalel, M., Adoko, A., & Korigov, S. (2020). *An approach to stope stability assessment in open stope mining environment.* Paper presented at the 54th US Rock Mechanics/Geomechanics Symposium.

APPENDIX A

Table 1. Data set for ELOS calculation

Deposit	Name of the mining unit	Q'	A	B	C	HR, м	N	Conditions
Belkina	Panel 31	15.5	1	0.23	3.4	6.6	12.1	Unstable
Belkina	Panel 27	15.5	1	0.2	2.52	15.3	7.8	Caved
Bystrushenskaya	Block 12 Stope 1	18.9	1	0.2	8	5.5	30.3	Stable
Bystrushenskaya	Block 12 Stope 2	18.9	1	0.2	8	8.3	30.3	Stable
Bystrushenskaya	Block 15 Stope 1	18.9	1	0.2	7.48	9.8	28.3	Stable
Bystrushenskaya	Block 16 Stope 1	19.7	1	0.2	7.48	12	29.5	Stable
Bystrushenskaya	Block 18 Stope 1	18.9	1	0.2	8	8.2	30.3	Stable
Bystrushenskaya	Block 5 Stope 3	18.9	1	0.2	7.48	4.1	28.3	Stable
Bystrushenskaya	Stope 5	18.9	1	0.2	8	8.7	30.3	Stable
Bystrushenskaya	Block 7 Stope 7	18.9	1	0.2	7.48	5.9	28.3	Stable
Pobeda	Block 28	16.3	1	0.2	2.65	15.2	8.6	Caved
Pobeda	Panel 85	16.3	1	0.4	2.09	19.5	13.7	Caved
Pobeda	Panel 94	16.3	1	0.2	2	6.8	6.5	Unstable
Pobeda	Panel 96	16.3	1	0.2	2	9.6	6.5	Unstable
Pobeda	Panel 100	16.3	1	0.2	2	14.2	6.5	Caved
Pobeda	Panel 107	16.3	1	0.2	2	21.2	6.5	Caved
Pobeda	Panel 84	9.1	0.28	0.33	2.65	9.3	2.2	Caved
Pobeda	Panel 37	16.3	1	0.2	2.8	11.9	9.1	Caved
Belkina	Panel 17	16.3	1	0.2	2	13.8	6.5	Caved
Belkina	Block 1	16.3	1	0.2	2	19	6.5	Caved
Belkina	Block 2	16.3	1	0.2	2	19	6.5	Caved
Belkina	Panel 11	18.9	1	0.2	2.09	6.4	7.9	Unstable
Belkina	Block 3	9.1	0.84	0.2	2.09	8.6	3.2	Unstable
Belkina	Panel 13	9.1	1	0.2	2.4	16.2	4.3	Caved
Belkina	Block 6	9.1	1	0.2	2.65	17.8	4.8	Caved
Belkina	Panel 20	16.3	1	0.2	2.33	14.5	7.6	Caved
Belkina	Panel 36	16.3	1	0.23	2.01	10.3	7.5	Caved
Belkina	Panel 33	16.3	1	0.23	2.01	8.9	7.5	Caved
Belkina	Block 4	9.1	0.96	0.2	3.27	9.5	5.7	Caved
Belkina	Panel 16	16.3	1	0.2	2.65	17.3	8.6	Caved
Belkina	Panel 21	9.1	1	0.2	2.09	9.2	3.8	Caved
Belkina	Panel 22	16.3	1	0.2	2.52	11.5	8.2	Caved
Belkina	Panel 24	15.5	1	0.2	4.56	11.1	14.1	Caved
Belkina	Panel 17	16.3	1	0.27	2	15.1	8.8	Caved
Perspektivnaya	Block 20	16.3	1	0.2	2.29	14.9	7.5	Caved

Perspektivnaya	Block 17 (North Wing)	16.3	1	0.2	2.09	13.2	6.8	Caved
Perspektivnaya	Block 17 (South Wing)	16.3	1	0.2	2.15	17.4	7	Caved
Perspektivnaya	Panel 17	16.3	1	0.2	2.48	9.351	8.1	Unstable
Perspektivnaya	Panel 18	16.3	1	0.2	2.48	9.032	8.1	Unstable
Perspektivnaya	Panel 11	9.1	1	0.28	2.56	11.3	6.5	Caved
Perspektivnaya	Panel 14	16.3	1	0.2	2.48	8.2	8.1	Caved
Pobeda	Panel 109	16.3	1	0.2	2.13	8.3	6.9	Unstable
Bystrushenskaya	Stope 36	15.5	1	0.2	8	19.6	24.7	Unstable
Belkina	Panel 1	16.3	1	0.2	2	11.6	6.5	Caved
Belkina	Panel 45	16.3	1	0.2	2	11.6	6.5	Caved
Belkina	Panel 35	16.3	1	0.2	3.09	12.13	10	Caved
Pobeda	Panel 60	15.5	1	0.2	2	8.6	6.2	Caved
Pobeda	Panel 46	16.3	1	0.2	2.29	9.3	7.5	Caved
Pobeda	Panel 47	16.3	1	0.2	2.2	7.7	7.2	Unstable
Pobeda	Panel 24	16.5	0.42	0.2	2.29	12.8	3.2	Caved
Pobeda	Panel 93	16.5	0.52	0.2	2.7	8.3	4.7	Caved
Pobeda	Panel 117	16.3	1	0.2	3.4	15.2	11.1	Caved
Pobeda	Panel 111	16.3	1	0.2	2.44	18.1	7.9	Caved
Pobeda	Panel 79	16.3	1	0.2	2.02	9.3	6.6	Unstable
Pobeda	Panel 81	16.3	1	0.2	2.2	11.1	7.2	Unstable
Pobeda	Panel 105	15.5	1	0.2	6.96	14.5	21.5	Unstable
Pobeda	Block 22	15.5	1	0.2	6.96	9.9	21.5	Unstable
Vtoraya Ridderskaya	Stope 2 Centre	9.1	1	0.2	5.46	5.2	9.9	Stable
Vtoraya Ridderskaya	Stope 2 East	18.9	1	0.23	3.47	5.2	15	Stable
Vtoraya Ridderskaya	Stope 3	18.9	1	0.28	4.14	5.3	21.6	Stable
Ridderskaya	Block 11 Stope 20	18.9	1	0.2	4.56	5.6	17.3	Stable
Bystrushenskaya	Block 15 Stope 2	18.9	1	0.2	7.48	9.5	28.3	Stable
Bystrushenskaya	Stope 23	18.9	1	0.2	3.21	5.9	12.1	Stable
Bystrushenskaya	Stope 22	18.9	1	0.2	7.48	7.1	28.3	Stable
Bystrushenskaya	Block 19 Stope 1	18.9	1	0.2	6.96	11.6	26.3	Stable
Bystrushenskaya	Block 19 Stope 2	18.9	1	0.2	7.27	11.1	27.5	Stable
Bystrushenskaya	Block 19 Stope 3	18.9	1	0.2	8	9.7	30.3	Stable
Bystrushenskaya	Block 19 Stope 5	18.9	1	0.2	8	5.2	30.3	Stable
Bystrushenskaya	Block 9 Stope 1	18.9	1	0.2	6.96	9.5	26.3	Stable
Bystrushenskaya	Block 9 Stope 2	18.9	1	0.2	8	7.7	30.3	Stable
Bystrushenskaya	Block 12 Stope 3	18.9	1	0.2	6.96	5.9	26.3	Stable
Bystrushenskaya	Block 12 Stope 1	18.9	1	0.2	8	5.5	30.3	Stable

Bystrushenskaya	Block 3 Stope 4	18.9	1	0.2	6.96	7.4	26.3	Stable
Bystrushenskaya	Block 3 Stope 4	18.9	1	0.23	3.4	5.8	14.9	Stable
Bystrushenskaya	Block 12 Stope 4	18.9	1	0.2	6.96	6.3	26.3	Stable
Bystrushenskaya	Block 12 Stope 2	18.9	1	0.2	8	8.3	30.3	Stable
Bystrushenskaya	Block 5 Stope 1	18.9	1	0.2	8	9.4	30.3	Stable
Bystrushenskaya	Block 5 Stope 2	18.9	1	0.2	8	6	30.3	Stable
Bystrushenskaya	Block 5 Stope 3	18.9	1	0.2	7.48	11.2	28.3	Stable
Bystrushenskaya	Block 5 Stope 4	18.9	1	0.2	8	11.6	30.3	Stable
Bystrushenskaya	Block 5 Stope 5	18.9	1	0.2	6.96	4.4	26.3	Stable
Bystrushenskaya	Block 5 Stope 6	18.9	1	0.2	8	7	30.3	Stable
Bystrushenskaya	Block 5 Stope 7	18.9	1	0.2	7.48	9.5	28.3	Stable
Bystrushenskaya	Block 5 Stope 8	18.9	1	0.2	7.48	6.1	28.3	Stable
Bystrushenskaya	Block 5 Stope 10	18.9	1	0.2	7.48	4.1	28.3	Stable
Bystrushenskaya	Block 5 Stope 11	18.9	1	0.2	7.06	5.3	26.7	Stable
Bystrushenskaya	Block 7 Stope 3	18.9	1	0.2	2.09	8.3	7.9	Stable
Bystrushenskaya	Block 7 Stope 6	18.9	1	0.2	6.96	8.7	26.3	Stable
Perspektivnaya	Block 16	16.3	1	0.2	2.2	16.7	7.2	Caved
Perspektivnaya	Panel 50	15.5	1	0.2	2.2	7	6.8	Stable
Perspektivnaya	Panel 51	15.5	1	0.2	2.2	22.6	6.8	Caved
Belkina	Panel 39	16.3	1	0.2	2.8	9.6	9.1	Caved
Bystrushenskaya	Block 11	16.3	1	0.2	5.66	10.5	18.4	Stable
Perspektivnaya	Block 22	16.3	1	0.2	2.11	17	6.9	Caved
Belkina	Panel 12	16.3	1	0.2	2.13	11.4	6.9	Caved
Belkina	Panel 3	16.3	1	0.2	2.15	10.53	7	Caved
Belkina	Panel 9	16.3	1	0.2	2.15	10.025	7	Caved
Belkina	Panel 14	9.1	1	0.2	2.4	12.7	4.3	Caved
Belkina	Panel 13	9.1	1	0.2	2.4	16	4.3	Caved
Belkina	Block 3	9.1	1	0.2	2.4	8.6	4.3	Caved
Belkina	Panel 23	16.3	1	0.3	2	22.5	9.8	Caved
Perspektivnaya	Panel 25	16.3	1	0.2	2.23	14.2	7.3	Caved
Pobeda	Panel 105	15.5	1	0.2	2.04	7.23	6.3	Unstable
Pobeda	Panel 97	15.5	1	0.2	2.04	11.7	6.3	Unstable
Bystrushenskaya	Block 95 Stope 8	15.5	1	0.2	5.28	11.5	16.3	Unstable
Bystrushenskaya	Block 95 Stope 10	15.5	0.68	0.2	5.28	11.5	11.1	Unstable
Bystrushenskaya	Block 95 Stope 11	15.5	0.59	0.2	5.28	10.9	9.6	Unstable

Table 2. ELOS results

Deposit	Name of the mining unit	Actual Dilution (%)	Stope/ Orebody width	Actual ELOS value	Expected ELOS Class	Actual Class	Difference
Belkina	Panel 31	13.60%	2.49	0.34	2	1	Different
Belkina	Panel 27	19.90%	2.49	0.5	4	1	Different
Bystrushenskaya	Block 12 Stope 1	23.10%	2.54	0.59	1	2	Different
Bystrushenskaya	Block 12 Stope 2	28.20%	2.54	0.72	1	2	Different
Bystrushenskaya	Block 15 Stope 1	14%	2.54	0.36	2	1	Different
Bystrushenskaya	Block 16 Stope 1	24.20%	2.54	0.61	2	2	Same
Bystrushenskaya	Block 18 Stope 1	17.70%	2.54	0.45	1	1	Same
Bystrushenskaya	Block 5 Stope 3	32.80%	2.54	0.83	1	2	Different
Bystrushenskaya	Stope 5	36.90%	2.54	0.94	2	2	Same
Bystrushenskaya	Block 7 Stope 7	24.10%	2.54	0.61	1	2	Different
Pobeda	Block 28	32.70%	2.55	0.83	4	2	Different
Pobeda	Panel 85	9.80%	2.55	0.25	4	1	Different
Pobeda	Panel 94	10.50%	2.55	0.27	3	1	Different
Pobeda	Panel 96	10%	2.55	0.26	3	1	Different
Pobeda	Panel 100	24.90%	2.55	0.63	4	2	Different
Pobeda	Panel 107	10%	2.55	0.26	5	1	Different
Pobeda	Panel 84	16.10%	2.55	0.41	4	1	Different
Pobeda	Panel 37	25%	2.55	0.64	3	2	Different
Belkina	Panel 17	19.80%	2.49	0.49	4	1	Different
Belkina	Block 1	5.80%	2.49	0.14	5	1	Different
Belkina	Block 2	5.80%	2.49	0.14	5	1	Different
Belkina	Panel 11	47%	2.49	1.17	2	3	Different
Belkina	Block 3	31.40%	2.49	0.78	4	2	Different
Belkina	Panel 13	13.50%	2.49	0.34	5	1	Different
Belkina	Block 6	17.70%	2.49	0.44	5	1	Different
Belkina	Panel 20	11.70%	2.49	0.29	4	1	Different
Belkina	Panel 36	25.30%	2.49	0.63	3	2	Different
Belkina	Panel 33	9.40%	2.49	0.23	3	1	Different
Belkina	Block 4	34.70%	2.49	0.86	3	2	Different
Belkina	Panel 16	36.70%	2.49	0.91	5	2	Different
Belkina	Panel 21	28.10%	2.49	0.7	4	2	Different
Belkina	Panel 22	29.10%	2.49	0.72	3	2	Different
Belkina	Panel 24	36.50%	2.49	0.91	3	2	Different
Belkina	Panel 17	19.80%	2.49	0.49	4	1	Different
Perspektivnaya	Block 20	36%	2.34	0.84	4	2	Different

Perspektivnaya	Block 17 (North Wing)	9%	2.34	0.21	4	1	Different
Perspektivnaya	Block 17 (South Wing)	1.10%	2.34	0.03	5	1	Different
Perspektivnaya	Panel 17	10.30%	2.34	0.24	3	1	Different
Perspektivnaya	Panel 18	14.40%	2.34	0.34	3	1	Different
Perspektivnaya	Panel 11	30%	2.34	0.7	4	2	Different
Perspektivnaya	Panel 14	23%	2.34	0.54	3	2	Different
Pobeda	Panel 109	10.30%	2.55	0.26	3	1	Different
Bystrushenskaya	Stope 36	13.10%	2.54	0.33	4	1	Different
Belkina	Panel 1	28%	2.49	0.7	4	2	Different
Belkina	Panel 45	17.30%	2.49	0.43	4	1	Different
Belkina	Panel 35	23.30%	2.49	0.58	3	2	Different
Pobeda	Panel 60	27.60%	2.55	0.7	3	2	Different
Pobeda	Panel 46	28.70%	2.55	0.73	3	2	Different
Pobeda	Panel 47	9.30%	2.55	0.24	3	1	Different
Pobeda	Panel 24	11%	2.55	0.28	5	1	Different
Pobeda	Panel 93	26.70%	2.55	0.68	3	2	Different
Pobeda	Panel 117	17.80%	2.55	0.45	4	1	Different
Pobeda	Panel 111	29.10%	2.55	0.74	5	2	Different
Pobeda	Panel 79	20.50%	2.55	0.52	3	2	Different
Pobeda	Panel 81	15.80%	2.55	0.4	3	1	Different
Pobeda	Panel 105	18.60%	2.55	0.47	3	1	Different
Pobeda	Block 22	31.40%	2.55	0.8	2	2	Same
Vtoraya Ridderskaya	Stope 2 Centre	20.20%	2.73	0.55	1	2	Different
Vtoraya Ridderskaya	Stope 2 East	20.20%	2.73	0.55	1	2	Different
Vtoraya Ridderskaya	Stope 3	20.20%	2.73	0.55	1	2	Different
Ridderskaya	Block 11 Stope 20	14.60%	2.5	0.37	1	1	Same
Bystrushenskaya	Block 15 Stope 2	38.50%	2.54	0.98	2	2	Same
Bystrushenskaya	Stope 23	47.20%	2.54	1.2	1	3	Different
Bystrushenskaya	Stope 22	26.90%	2.54	0.68	1	2	Different
Bystrushenskaya	Block 19 Stope 1	24.10%	2.54	0.61	3	2	Different
Bystrushenskaya	Block 19 Stope 2	27.20%	2.54	0.69	2	2	Same
Bystrushenskaya	Block 19 Stope 3	35.60%	2.54	0.9	2	2	Same
Bystrushenskaya	Block 19 Stope 5	24.80%	2.54	0.63	1	2	Different
Bystrushenskaya	Block 9 Stope 1	21%	2.54	0.53	2	2	Same
Bystrushenskaya	Block 9 Stope 2	21.20%	2.54	0.54	1	2	Different
Bystrushenskaya	Block 12 Stope 3	21.10%	2.54	0.54	1	2	Different
Bystrushenskaya	Block 12 Stope 1	21.10%	2.54	0.54	1	2	Different

Bystrushenskaya	Block 3 Stope 4	8.80%	2.54	0.22	1	1	Same
Bystrushenskaya	Block 3 Stope 4	16.20%	2.54	0.41	1	1	Same
Bystrushenskaya	Block 12 Stope 4	16.20%	2.54	0.41	1	1	Same
Bystrushenskaya	Block 12 Stope 2	34%	2.54	0.86	1	2	Different
Bystrushenskaya	Block 5 Stope 1	28.20%	2.54	0.72	2	2	Same
Bystrushenskaya	Block 5 Stope 2	25%	2.54	0.64	1	2	Different
Bystrushenskaya	Block 5 Stope 3	17.30%	2.54	0.44	2	1	Different
Bystrushenskaya	Block 5 Stope 4	16.50%	2.54	0.42	2	1	Different
Bystrushenskaya	Block 5 Stope 5	10%	2.54	0.25	1	1	Same
Bystrushenskaya	Block 5 Stope 6	9.60%	2.54	0.24	1	1	Same
Bystrushenskaya	Block 5 Stope 7	10.40%	2.54	0.26	2	1	Different
Bystrushenskaya	Block 5 Stope 8	13.10%	2.54	0.33	1	1	Same
Bystrushenskaya	Block 5 Stope 10	9.60%	2.54	0.24	1	1	Same
Bystrushenskaya	Block 5 Stope 11	32.80%	2.54	0.83	1	2	Different
Bystrushenskaya	Block 7 Stope 3	21.30%	2.54	0.54	3	2	Different
Bystrushenskaya	Block 7 Stope 6	32.30%	2.54	0.82	2	2	Same
Perspektivnaya	Block 16	36%	2.34	0.84	5	2	Different
Perspektivnaya	Panel 50	5.30%	2.34	0.12	3	1	Different
Perspektivnaya	Panel 51	15.80%	2.34	0.37	5	1	Different
Belkina	Panel 39	14.80%	2.49	0.37	3	1	Different
Bystrushenskaya	Block 11	17.80%	2.54	0.45	3	1	Different
Perspektivnaya	Block 22	24.30%	2.34	0.57	5	2	Different
Belkina	Panel 12	25.40%	2.49	0.63	4	2	Different
Belkina	Panel 3	23%	2.49	0.57	3	2	Different
Belkina	Panel 9	33.90%	2.49	0.84	3	2	Different
Belkina	Panel 14	14.70%	2.49	0.37	5	1	Different
Belkina	Panel 13	13.50%	2.49	0.34	5	1	Different
Belkina	Block 3	31.40%	2.49	0.78	3	2	Different
Belkina	Panel 23	8.50%	2.49	0.21	5	1	Different
Perspektivnaya	Panel 25	23.30%	2.34	0.55	4	2	Different
Pobeda	Panel 105	18.60%	2.55	0.47	3	1	Different
Pobeda	Panel 97	28.80%	2.55	0.73	4	2	Different
Bystrushenskaya	Block 95 Stope 8	53.50%	2.54	1.36	3	3	Same
Bystrushenskaya	Block 95 Stope 10	56.10%	2.54	1.42	3	3	Same
Bystrushenskaya	Block 95 Stope 11	2%	2.54	0.05	3	1	Different

APPENDIX B

Table 1. Multinomial Regression Analysis parameters

HR, m	N	Major, Moderate and Minor				Major and Minor		
		P1	P2	P3	SUM	P1	P2	SUM
6.6	12.1	0.325303	0.411355	0.263343	1	0.356727	0.643273	1
15.3	7.8	0.309055	0.310014	0.380931	1	0.599096	0.400904	1
5.5	30.3	0.426846	0.383609	0.189545	1	0.2908	0.7092	1
8.3	30.3	0.435293	0.3527	0.212007	1	0.357484	0.642516	1
9.8	28.3	0.426642	0.341055	0.232303	1	0.40064	0.59936	1
12	29.5	0.438082	0.31479	0.247128	1	0.456361	0.543639	1
8.2	30.3	0.435028	0.353792	0.21118	1	0.354985	0.645015	1
4.1	28.3	0.410136	0.404839	0.185025	1	0.26423	0.73577	1
8.7	30.3	0.436324	0.348342	0.215333	1	0.36756	0.63244	1
5.9	28.3	0.416281	0.384429	0.19929	1	0.304089	0.695911	1
15.2	8.6	0.313631	0.31051	0.37586	1	0.594548	0.405452	1
19.5	13.7	0.340389	0.25824	0.401372	1	0.690081	0.309919	1
6.8	6.5	0.295751	0.417555	0.286694	1	0.374772	0.625228	1
9.6	6.5	0.299749	0.381552	0.318699	1	0.448533	0.551467	1
14.2	6.5	0.302006	0.32426	0.373734	1	0.573171	0.426829	1
21.2	6.5	0.295178	0.244613	0.460208	1	0.74227	0.25773	1
9.3	2.2	0.276885	0.390061	0.333054	1	0.451082	0.548918	1
11.9	9.1	0.315938	0.349725	0.334336	1	0.504525	0.495475	1
13.8	6.5	0.302026	0.329116	0.368858	1	0.562472	0.437528	1
19	6.5	0.298607	0.26844	0.432953	1	0.693812	0.306188	1
19	6.5	0.298607	0.26844	0.432953	1	0.693812	0.306188	1
6.4	7.9	0.30235	0.420686	0.276964	1	0.361375	0.638625	1
8.6	3.2	0.28128	0.398198	0.320522	1	0.429816	0.570184	1
16.2	4.3	0.28906	0.301851	0.409089	1	0.630602	0.369398	1
17.8	4.8	0.290447	0.282879	0.426674	1	0.669118	0.330882	1
14.5	7.6	0.308118	0.3197	0.372182	1	0.578471	0.421529	1
10.3	7.5	0.305863	0.371496	0.32264	1	0.464982	0.535018	1
8.9	7.5	0.304286	0.389229	0.306485	1	0.427294	0.572706	1
9.5	5.7	0.295369	0.383764	0.320867	1	0.447816	0.552184	1
17.3	8.6	0.312456	0.286221	0.401322	1	0.648328	0.351672	1
9.2	3.8	0.285052	0.389737	0.325211	1	0.444431	0.555569	1
11.5	8.2	0.310676	0.355687	0.333636	1	0.495875	0.504125	1
11.1	14.1	0.343735	0.35286	0.303406	1	0.47026	0.52974	1

15.1	8.8	0.314798	0.31151	0.373692	1	0.591435	0.408565	1
14.9	7.5	0.307478	0.31501	0.377512	1	0.589307	0.410693	1
13.2	6.8	0.303636	0.336174	0.360189	1	0.545573	0.454427	1
17.4	7	0.303212	0.286183	0.410605	1	0.654437	0.345563	1
9.351	8.1	0.308098	0.38273	0.309173	1	0.437887	0.562113	1
9.032	8.1	0.307696	0.386769	0.305536	1	0.429348	0.570652	1
11.3	6.5	0.301216	0.360045	0.338739	1	0.494675	0.505325	1
8.2	8.1	0.306526	0.397344	0.296131	1	0.407285	0.592715	1
8.3	6.9	0.300258	0.397677	0.302065	1	0.412825	0.587175	1
19.6	24.7	0.409638	0.245765	0.344597	1	0.668498	0.331502	1
11.6	6.5	0.301399	0.356286	0.342316	1	0.50285	0.49715	1
11.6	6.5	0.301399	0.356286	0.342316	1	0.50285	0.49715	1
12.13	10	0.321134	0.345865	0.333002	1	0.508542	0.491458	1
8.6	6.2	0.296952	0.394718	0.30833	1	0.42248	0.57752	1
9.3	7.5	0.304788	0.384143	0.311069	1	0.437996	0.562004	1
7.7	7.2	0.300947	0.404978	0.294075	1	0.396349	0.603651	1
12.8	3.2	0.284024	0.344212	0.371764	1	0.543688	0.456312	1
8.3	4.7	0.288675	0.400415	0.31091	1	0.418168	0.581832	1
15.2	11.1	0.328035	0.30816	0.363805	1	0.588508	0.411492	1
18.1	7.9	0.307674	0.277672	0.414653	1	0.669495	0.330505	1
9.3	6.6	0.299949	0.385258	0.314792	1	0.440212	0.559788	1
11.1	7.2	0.304897	0.361793	0.33331	1	0.487478	0.512522	1
14.5	21.5	0.390629	0.302705	0.306666	1	0.544259	0.455741	1
9.9	21.5	0.385626	0.354273	0.260101	1	0.419726	0.580274	1
5.2	9.9	0.310341	0.432841	0.256819	1	0.327349	0.672651	1
5.2	15	0.337884	0.423394	0.238723	1	0.31622	0.68378	1
5.3	21.6	0.375295	0.407896	0.216808	1	0.304428	0.695572	1
5.6	17.3	0.35173	0.413792	0.234478	1	0.320691	0.679309	1
9.5	28.3	0.425995	0.344339	0.229666	1	0.392814	0.607186	1
5.9	12.1	0.323755	0.42014	0.256105	1	0.339416	0.660584	1
7.1	28.3	0.419911	0.370941	0.209148	1	0.332456	0.667544	1
11.6	26.3	0.417581	0.325701	0.256718	1	0.453485	0.546515	1
11.1	27.5	0.424197	0.328652	0.247151	1	0.437061	0.562939	1
9.7	30.3	0.438706	0.337522	0.223772	1	0.393243	0.606757	1
5.2	30.3	0.425818	0.386957	0.187225	1	0.284103	0.715897	1
9.5	26.3	0.413804	0.348833	0.237363	1	0.397594	0.602406	1
7.7	30.3	0.433662	0.359267	0.207072	1	0.342607	0.657393	1
5.9	26.3	0.404456	0.389531	0.206014	1	0.308338	0.691662	1
7.4	26.3	0.408779	0.372439	0.218782	1	0.344253	0.655747	1
5.8	14.9	0.338865	0.416173	0.244962	1	0.330749	0.669251	1
6.3	26.3	0.405667	0.384957	0.209376	1	0.317713	0.682287	1
9.4	30.3	0.438021	0.340756	0.221222	1	0.385469	0.614531	1
6	30.3	0.428508	0.378044	0.193448	1	0.302167	0.697833	1
11.2	28.3	0.429317	0.325869	0.244813	1	0.437774	0.562226	1

11.6	30.3	0.442437	0.317284	0.240278	1	0.443591	0.556409	1
4.4	26.3	0.399549	0.406765	0.193686	1	0.274602	0.725398	1
7	30.3	0.431634	0.366969	0.201397	1	0.325634	0.674366	1
9.5	28.3	0.425995	0.344339	0.229666	1	0.392814	0.607186	1
6.1	28.3	0.416912	0.382174	0.200914	1	0.308722	0.691278	1
4.1	28.3	0.410136	0.404839	0.185025	1	0.26423	0.73577	1
5.3	26.7	0.404907	0.395384	0.199708	1	0.293738	0.706262	1
8.3	7.9	0.305601	0.396343	0.298056	1	0.410403	0.589597	1
8.7	26.3	0.412034	0.357776	0.23019	1	0.376906	0.623094	1
16.7	7.2	0.304913	0.294102	0.400986	1	0.636522	0.363478	1
7	6.8	0.297672	0.414549	0.287779	1	0.379187	0.620813	1
22.6	6.8	0.294151	0.230003	0.475846	1	0.769839	0.230161	1
9.6	9.1	0.313858	0.378283	0.307859	1	0.442111	0.557889	1
10.5	18.4	0.368143	0.353036	0.278821	1	0.443369	0.556631	1
17	6.9	0.302984	0.290842	0.406174	1	0.644741	0.355259	1
11.4	6.9	0.303462	0.358366	0.338172	1	0.4964	0.5036	1
10.53	7	0.303353	0.369181	0.327467	1	0.47247	0.52753	1
10.025	7	0.302883	0.375561	0.321556	1	0.458775	0.541225	1
12.7	4.3	0.289897	0.34458	0.365522	1	0.53825	0.46175	1
16	4.3	0.28919	0.30423	0.406581	1	0.625509	0.374491	1
8.6	4.3	0.286973	0.396981	0.316046	1	0.427123	0.572877	1
22.5	9.8	0.311908	0.229846	0.458247	1	0.762512	0.237488	1
14.2	7.3	0.306467	0.323568	0.369965	1	0.571213	0.428787	1
7.23	6.3	0.295442	0.412263	0.292295	1	0.386291	0.613709	1
11.7	6.3	0.300364	0.35524	0.344396	1	0.506075	0.493925	1
11.5	16.3	0.356985	0.344776	0.298239	1	0.475644	0.524356	1
11.5	11.1	0.326925	0.352175	0.3209	1	0.488627	0.511373	1
10.9	9.6	0.317985	0.361443	0.320571	1	0.476043	0.523957	1